Membranes

18.S995 - L16 & L17

dunkel@mit.edu

Cell membranes (D=2)

transport:
stochastic
escape problems

Illustration by J.P. Cartailler. Copyright 2007, Symmation LLC.

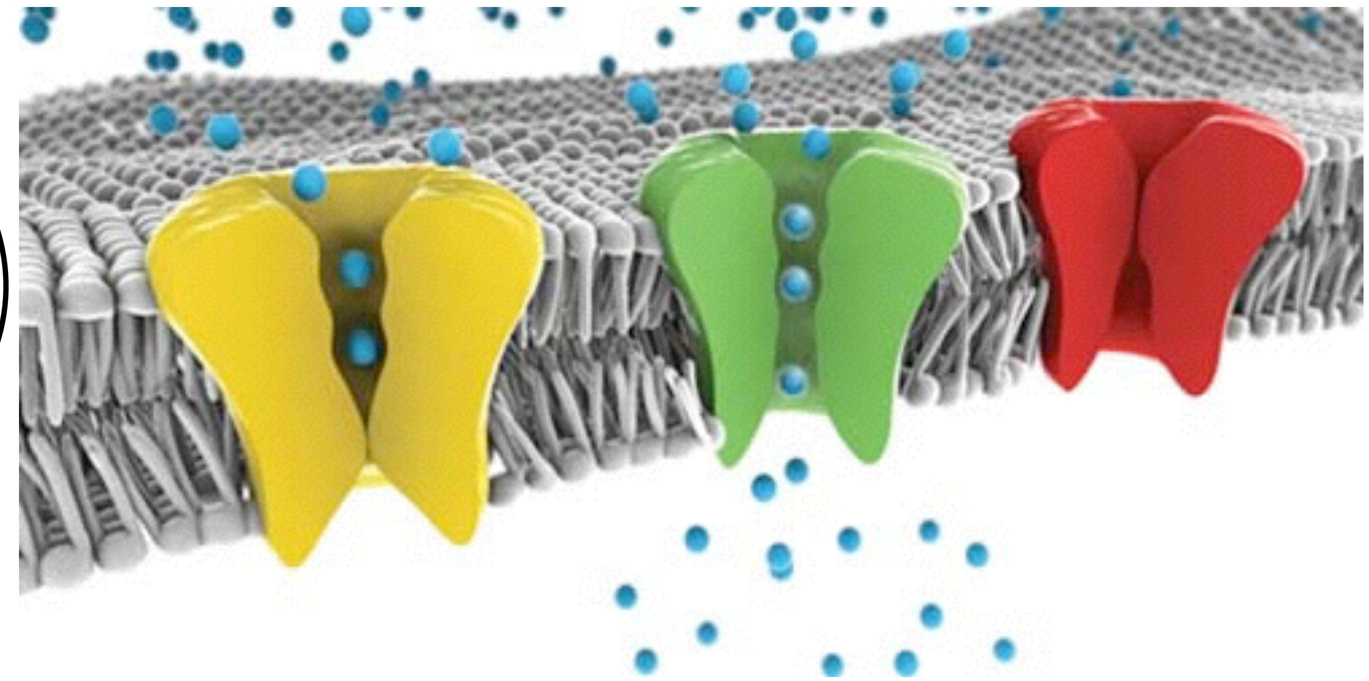

shape:
differential
geometry

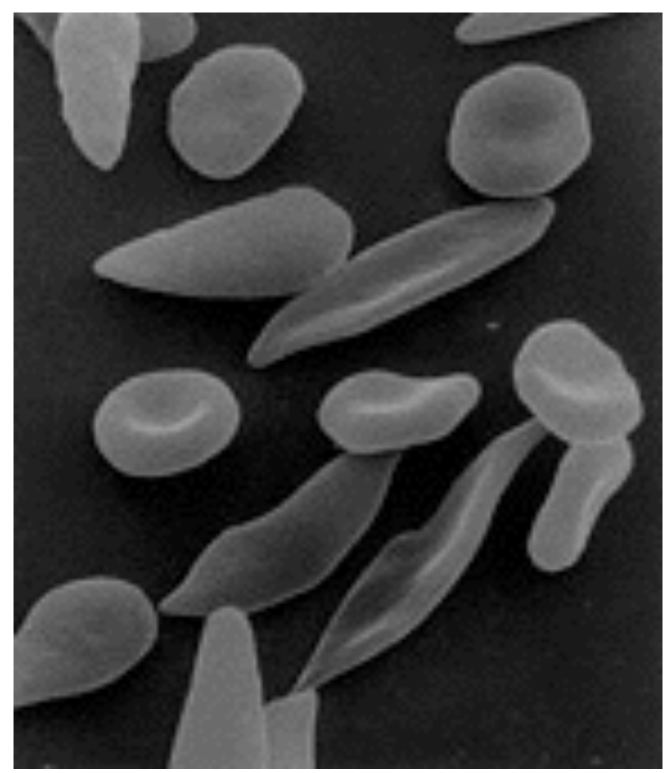

red blood cells
affected by
sickle-cell disease

source: wiki

dunkel@math.mit.edu

Cell membranes

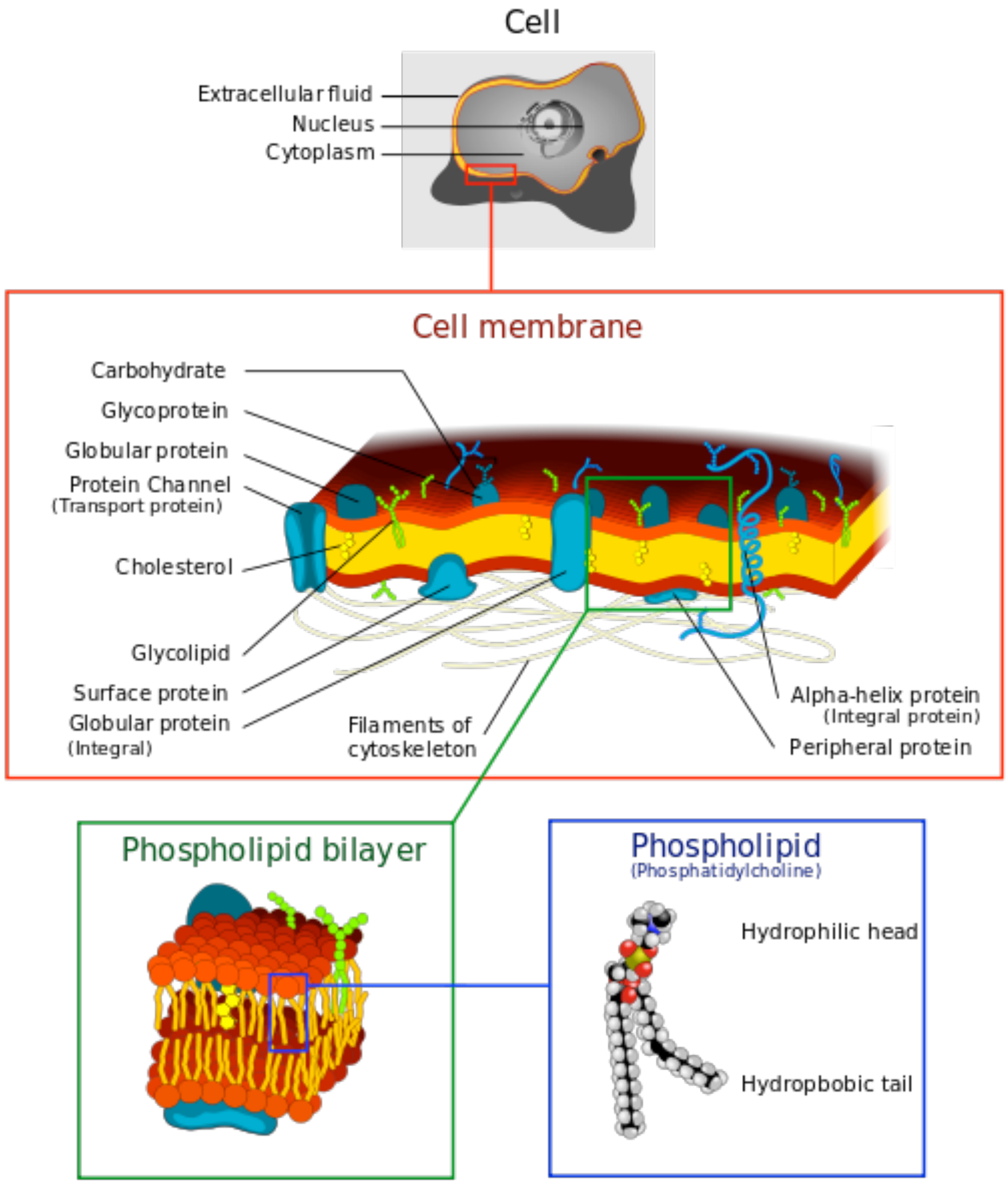

source: wiki

dunkel@math.mit.edu

AFM

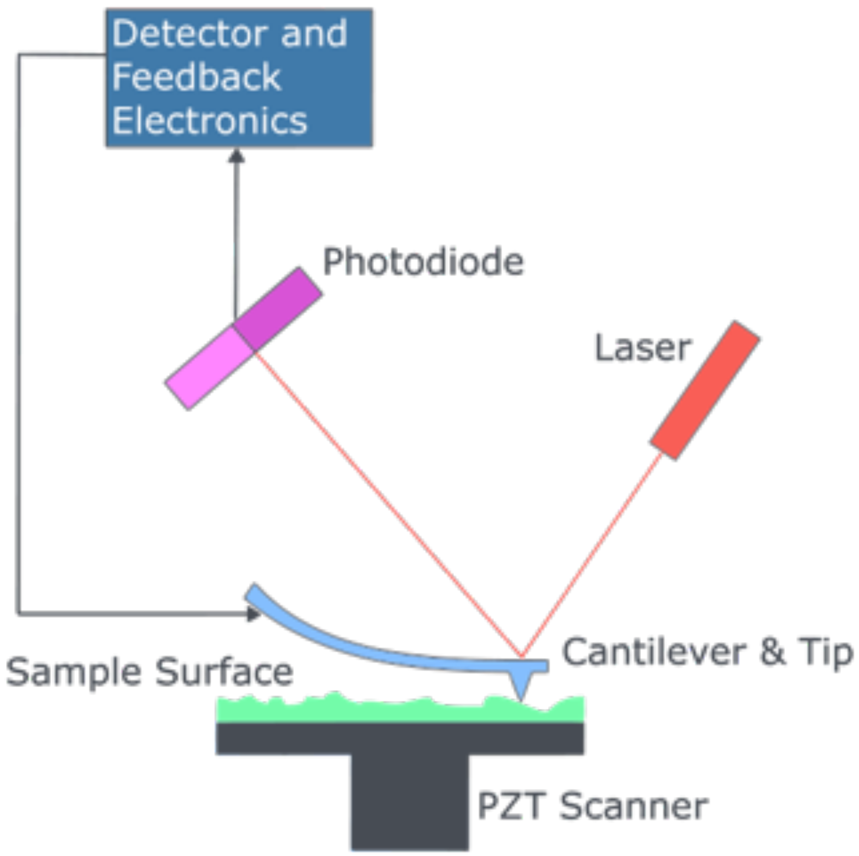

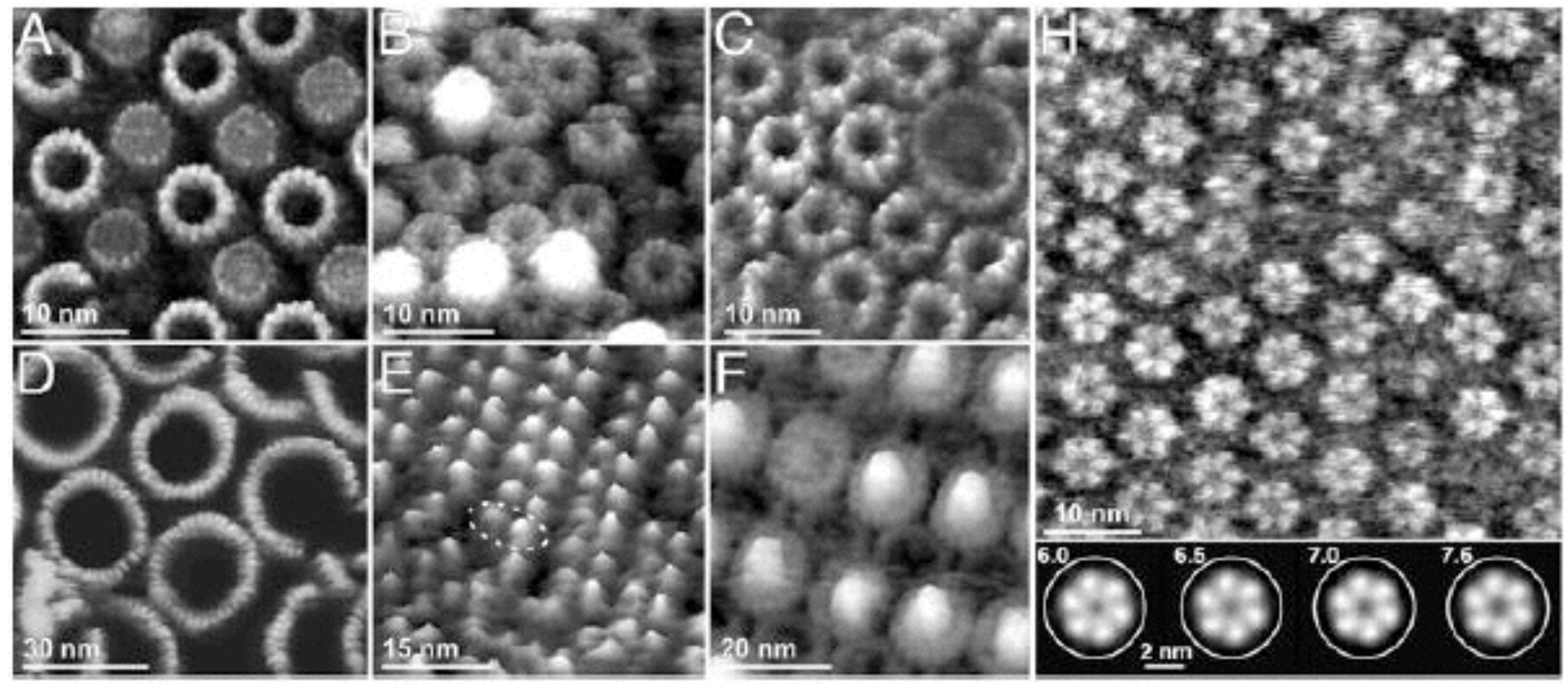

source: wiki

http://www.sbmp-itn.eu/sbmps/research_method/

Observing the oligomeric state, supramolecular assembly and function of native membrane proteins by AFM. (A) Proton-driven rotors from spinach chloroplast FoF1-ATP synthase [3]. (B) Sodium-driven rotors from *Ilyobacter tartaricus* FoF1-ATP synthase. (C) High-light-adapted native photosynthetic membrane from *Rsp. Photometricum*[3]. (D) Pore complexes of perfringolysin O (PFO), a prototype of the large family of pore-forming cholesterol-dependent cytolysins (CDCs). Image courtesy of Z. Shao (Virginia). (E) The oligomeric state of bovine rhodopsin in native disc membranes [3]. (F) Structrual organsiation of the light-harvesting complex I photosynthetic core complex of *Rsp. Rubrum* [3]. (H) Extracellular surface of gap junction hemichannels from rat liver Wells recorded at pH 7.6 [6]. In presence of aminosulfonate compounds the hemichannels open their channel entrance with increasing pH from the closed (pH 6.0) to open (pH 7.6).

Intercellular gap junctions

exchange of molecules and ions between animal cells

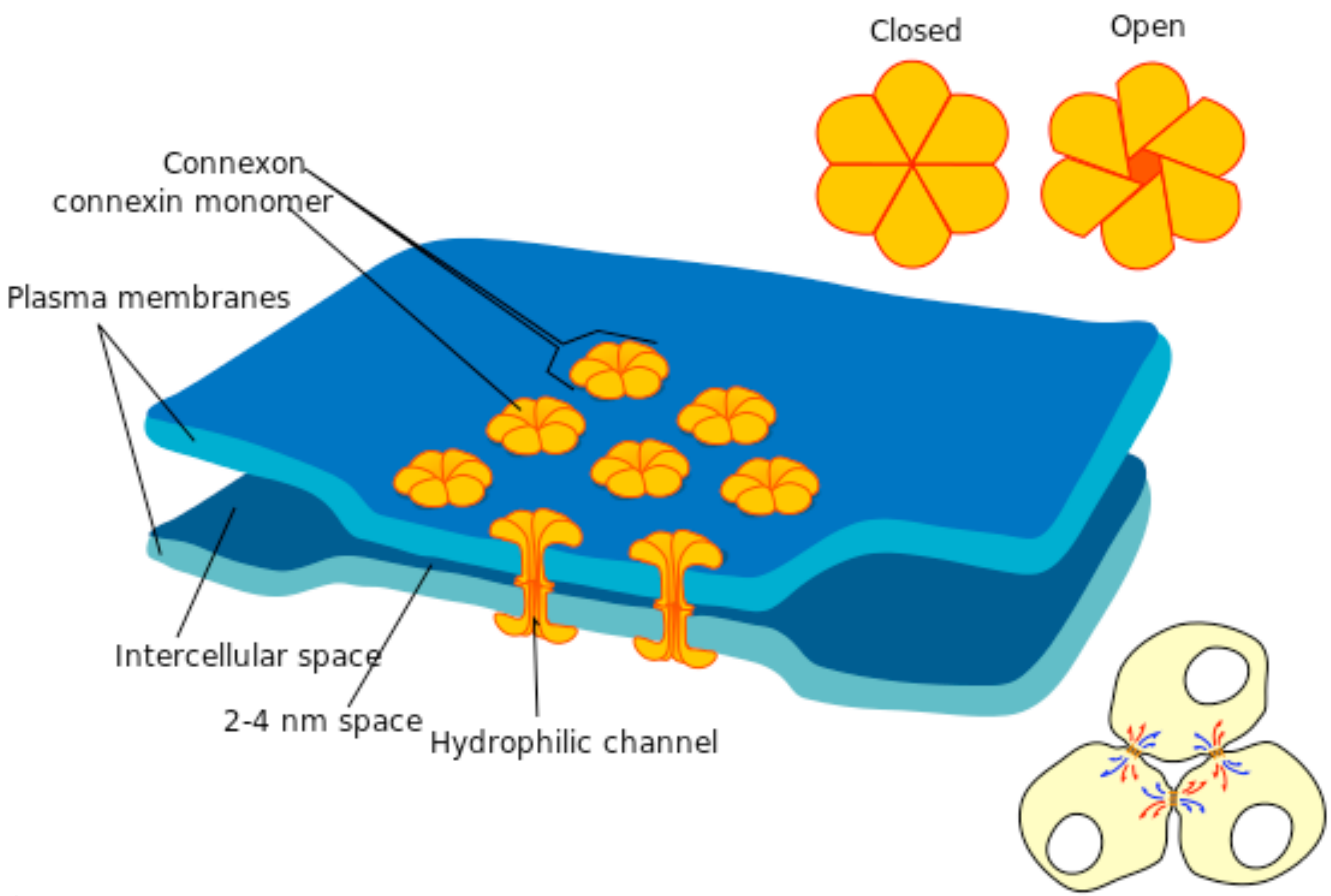

source: wiki

Active transport

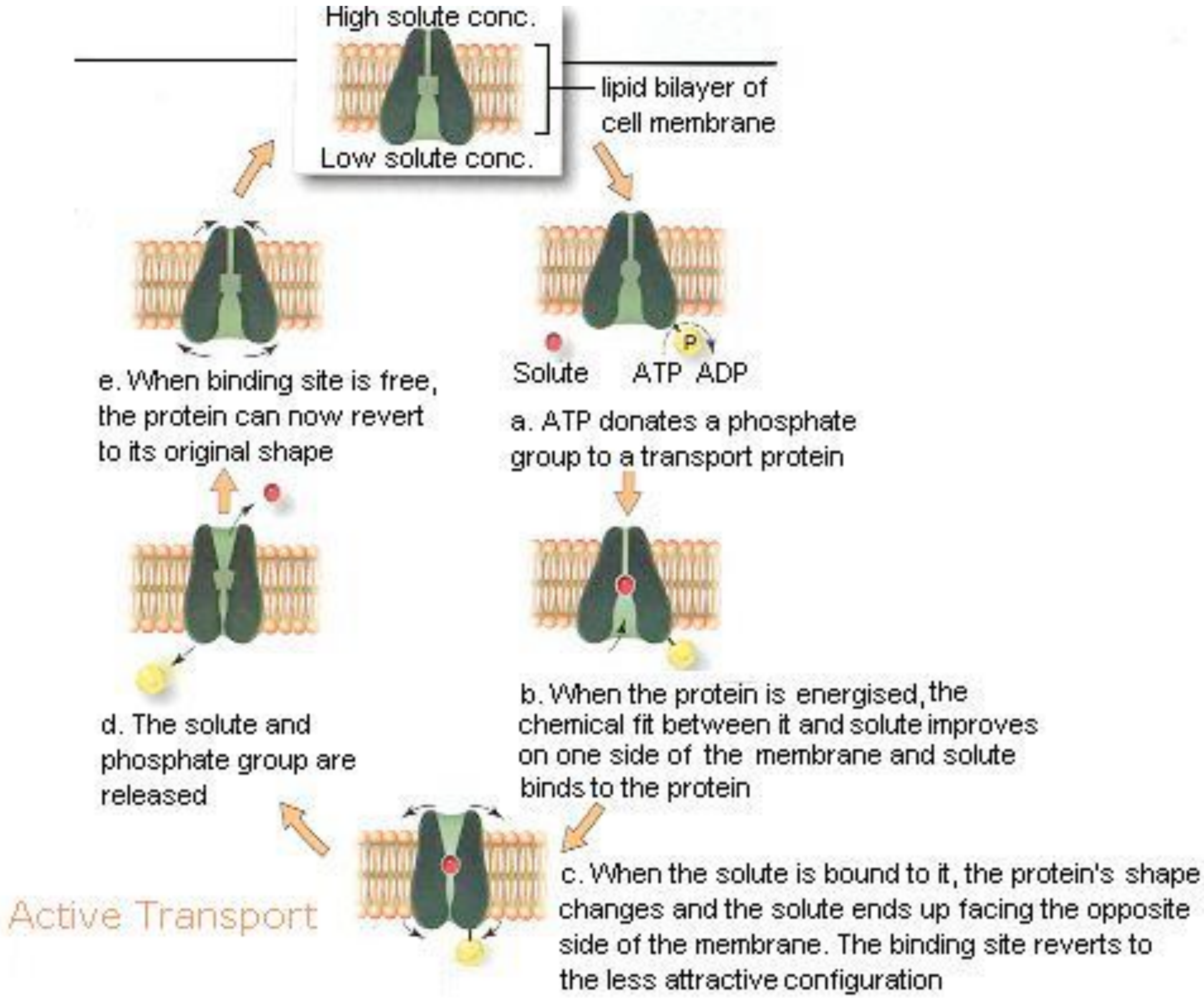

Bio-membrane

Selective barrier

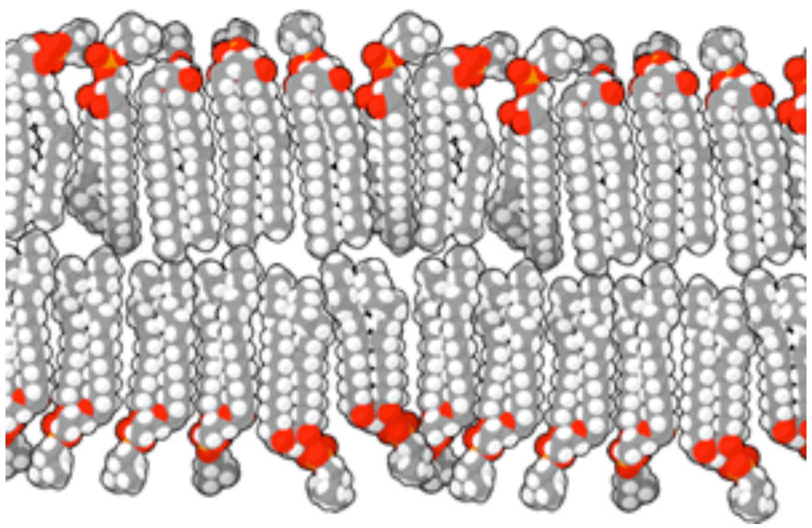

source: wiki

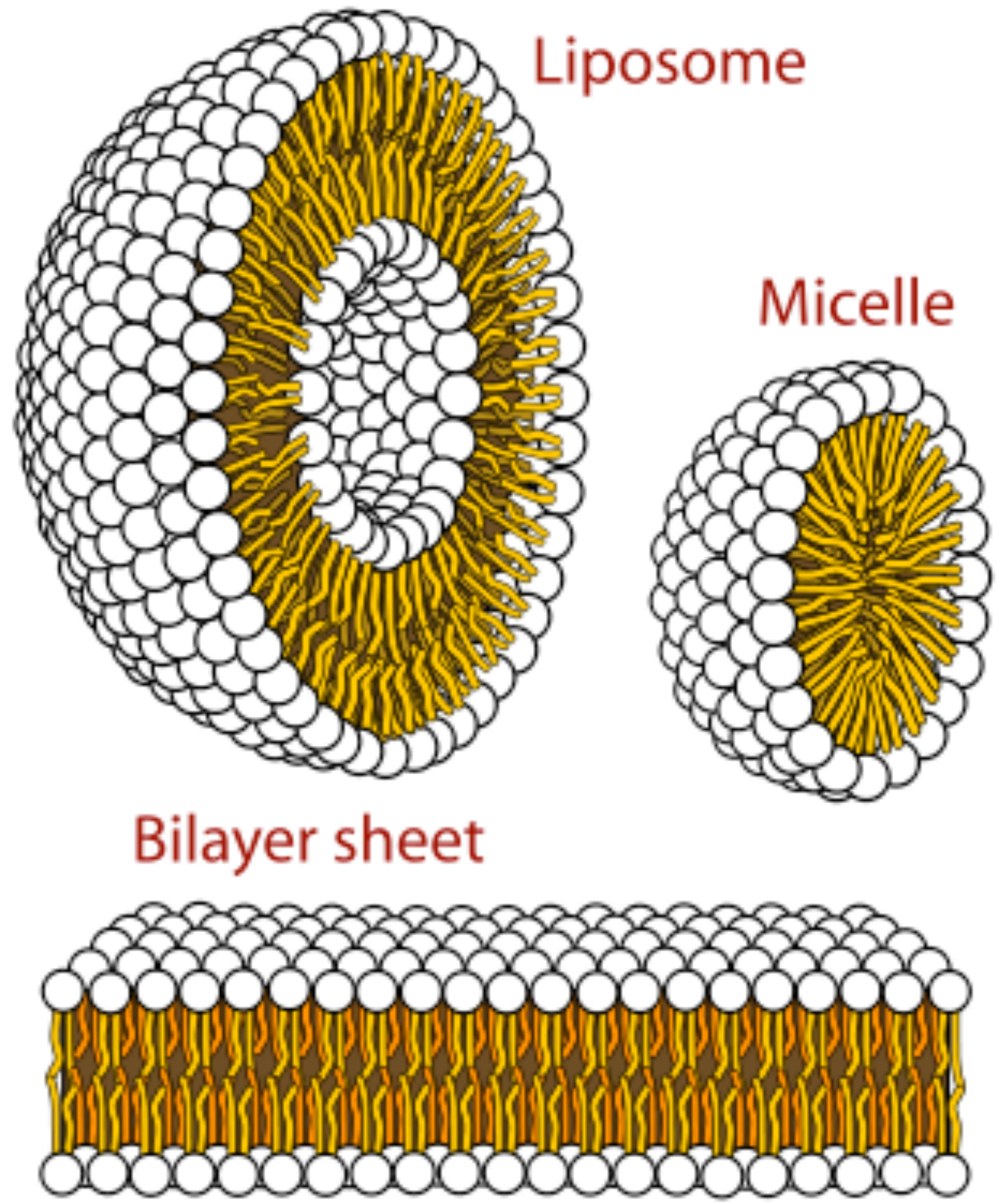

dunkel@math.mit.edu

Morphological changes

e.g., fusion through stalk-formation

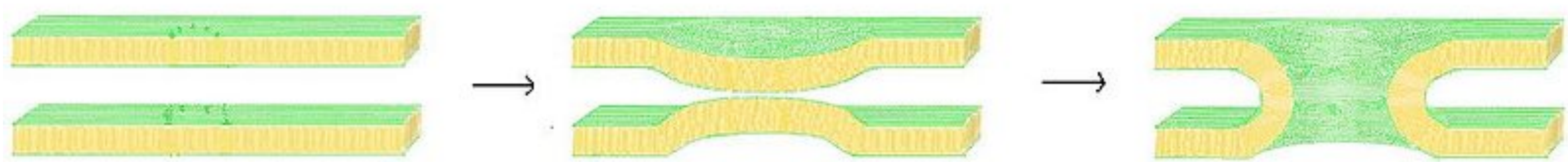

source: wiki

dunkel@math.mit.edu

Endo- & Exocytosis

material exchange with environment

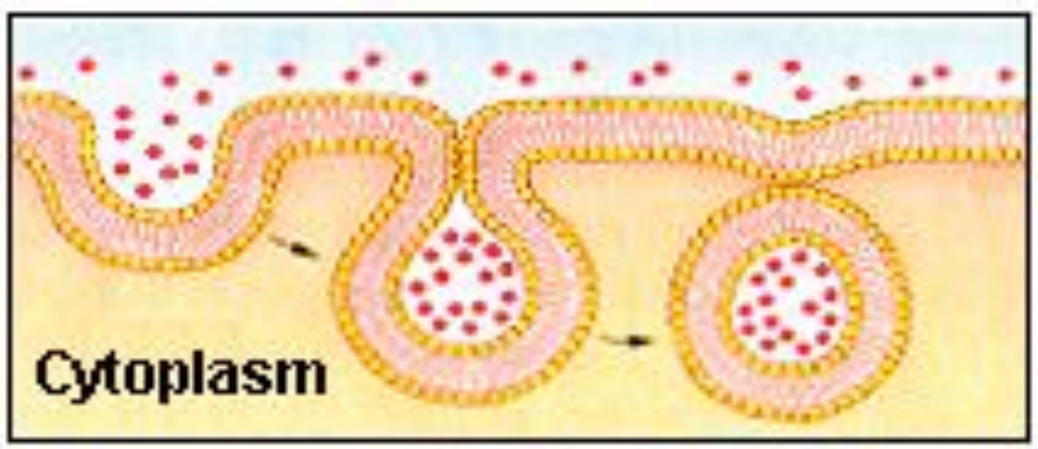

Endocytosis

A bit of plasma membrane baloons inwar
beneath water and solutes outside, then
pinches off as an endocytic vesicle that
moves into the cytoplasm

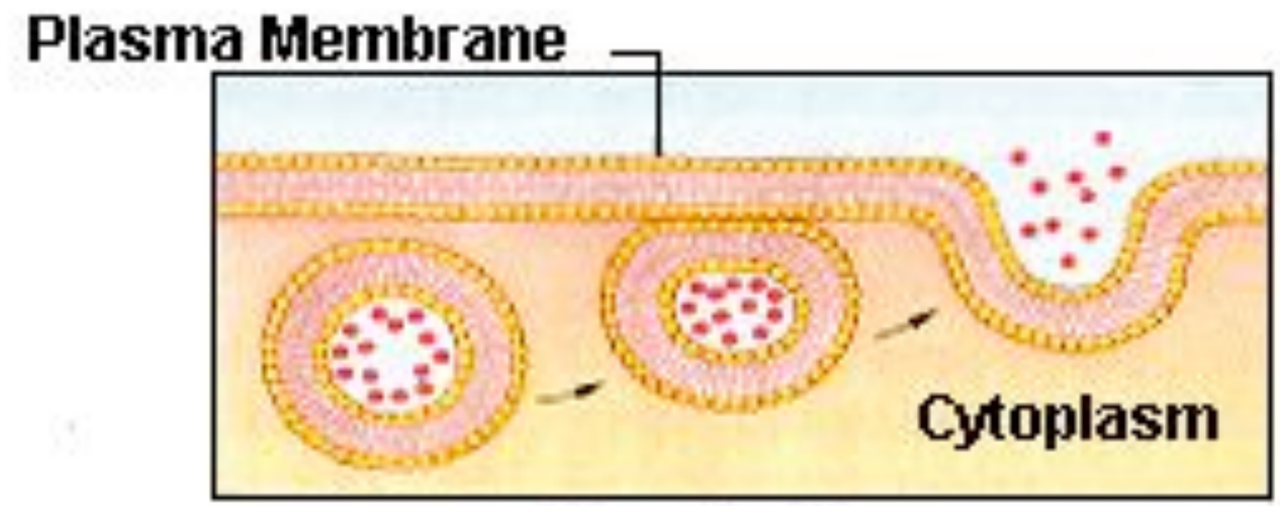

Exocytosis

Cells release substances when an
exocytic vesicle's membrane fuses
with the plasma membrane

dunkel@math.mit.edu

Virus envelop

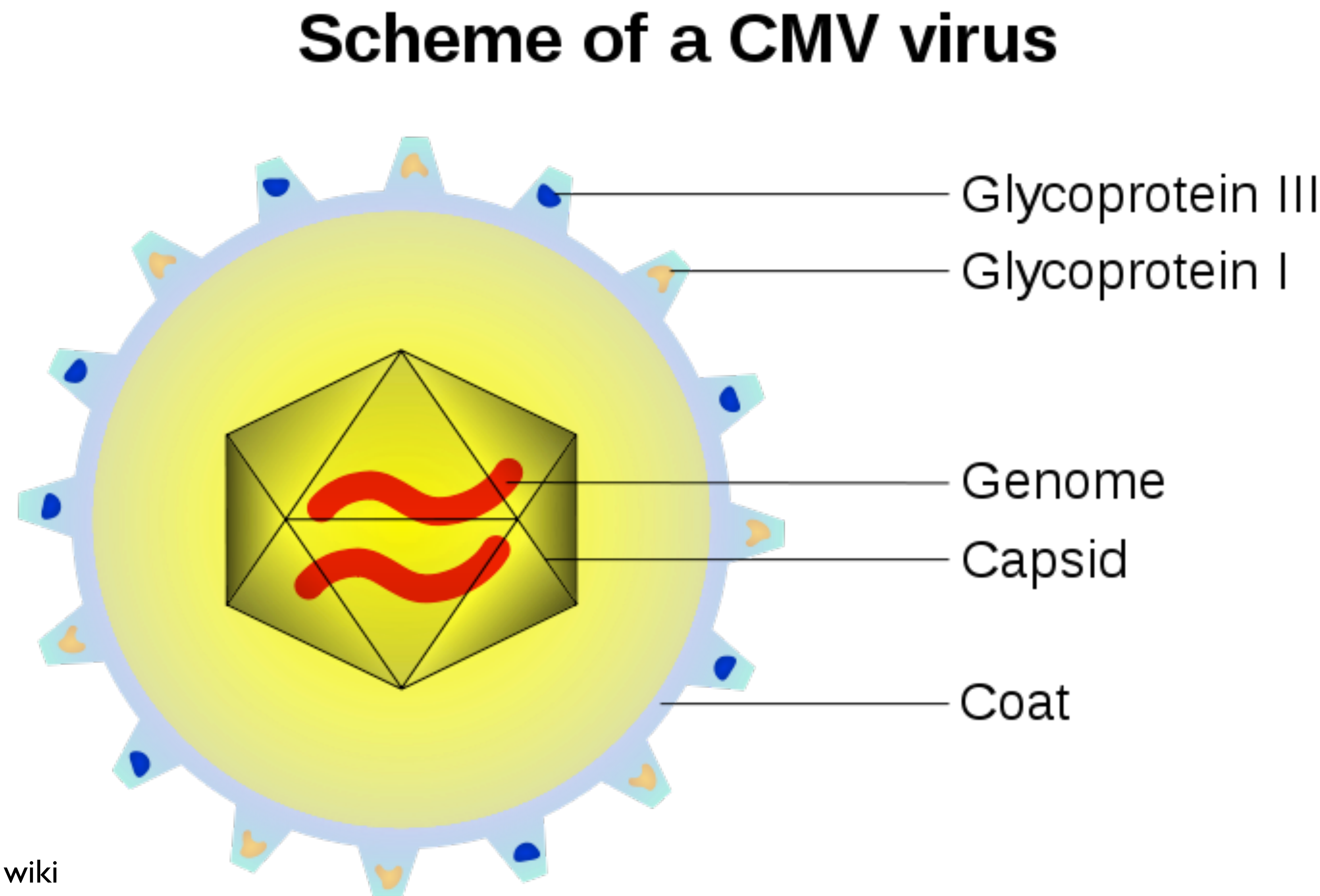

source: wiki

envelop fuses with host membrane

dunkel@math.mit.edu

Capsid

cryo-EM

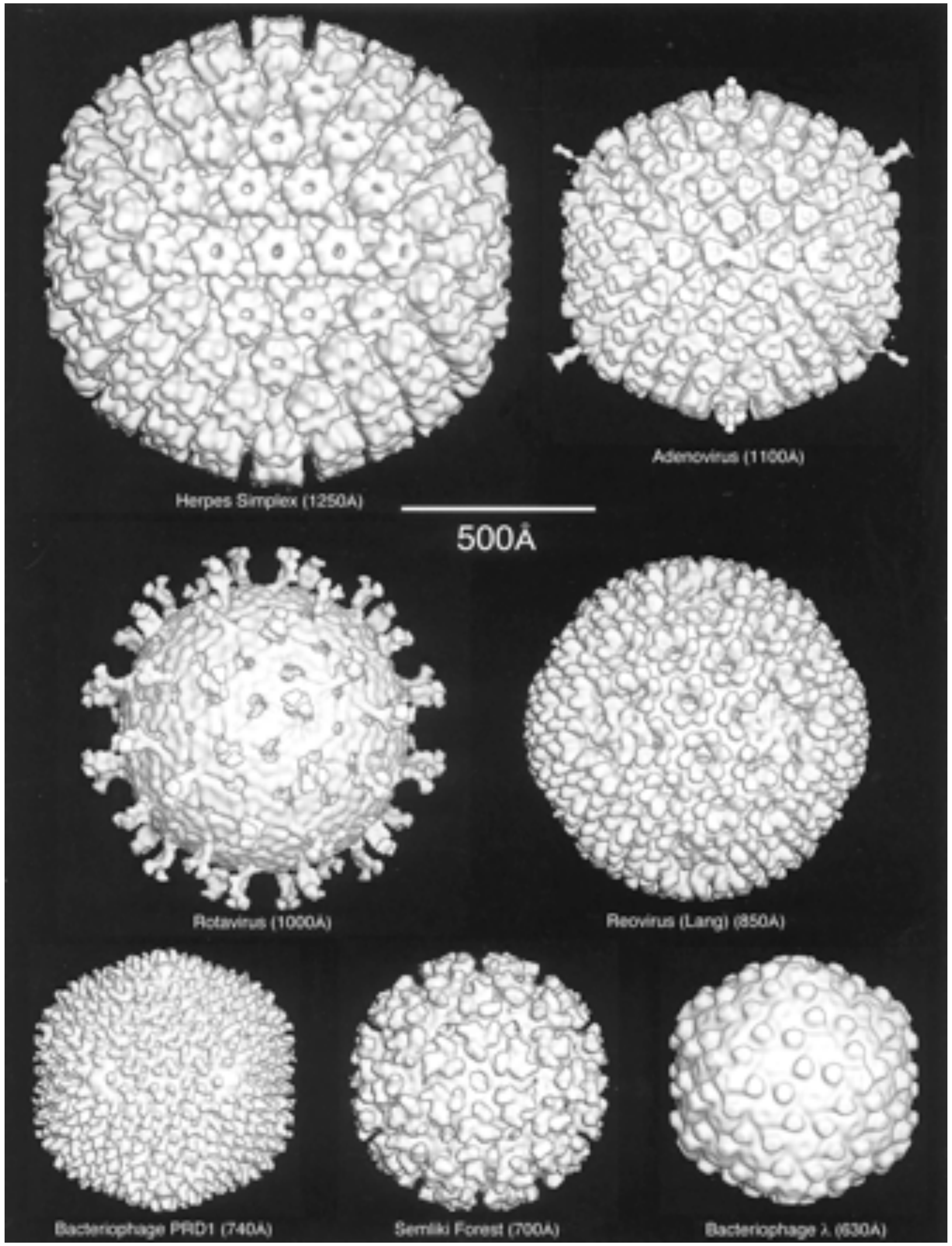

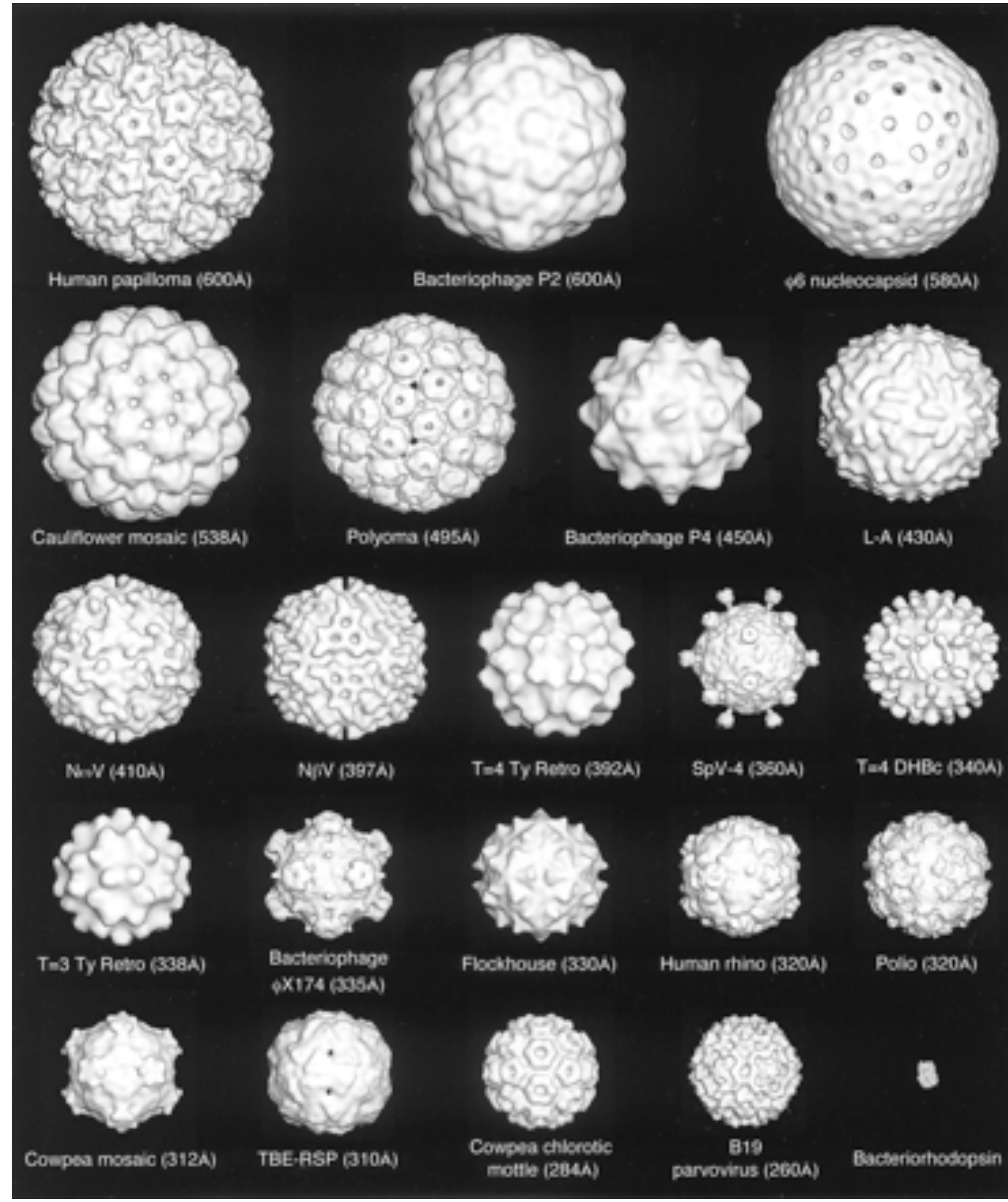

Baker et al (1999) MMBR

dunkel@math.mit.edu

Diatoms (algae)

H_4SiO_4

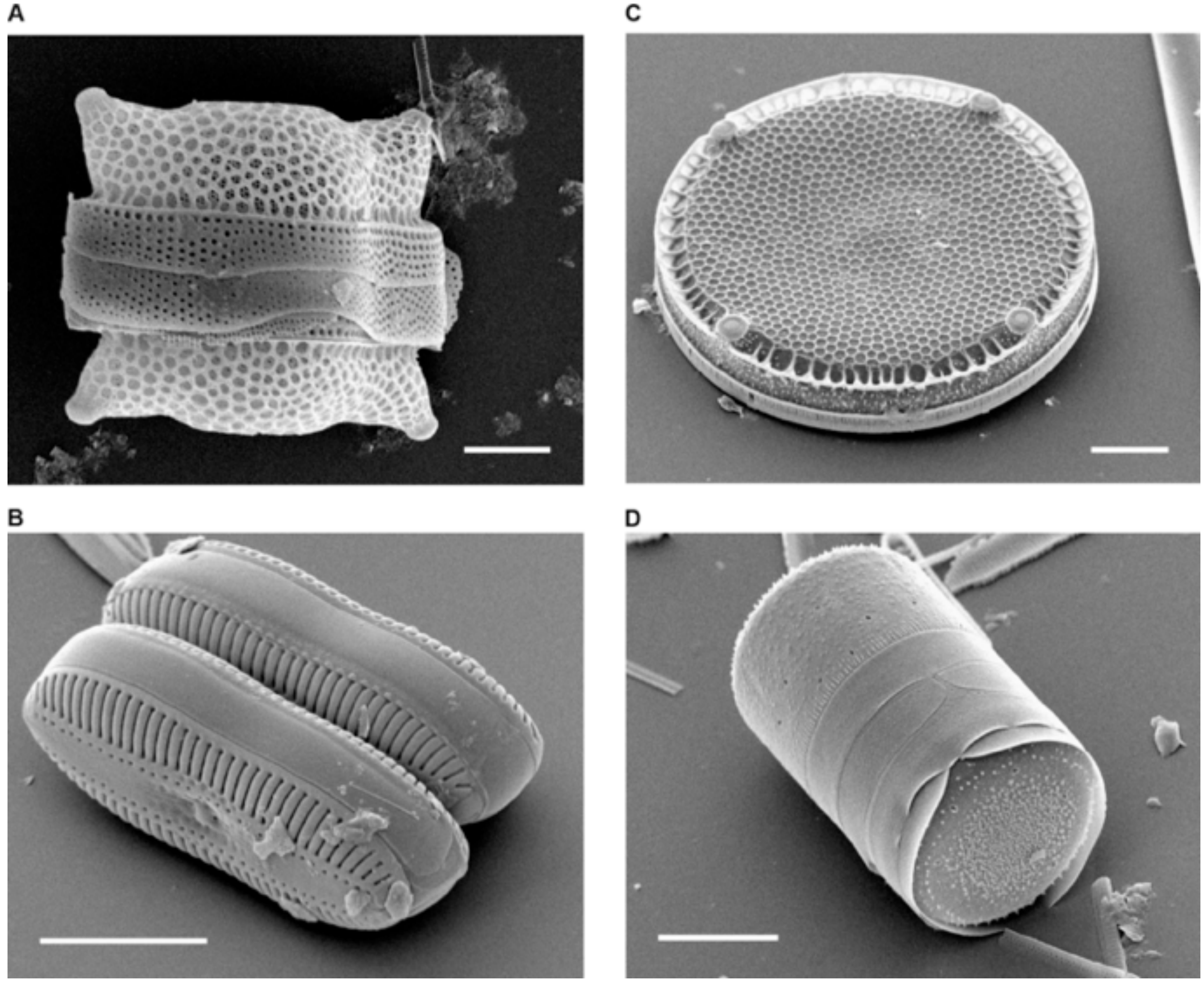

source: wiki

dunkel@math.mit.edu

More planktonic diatoms

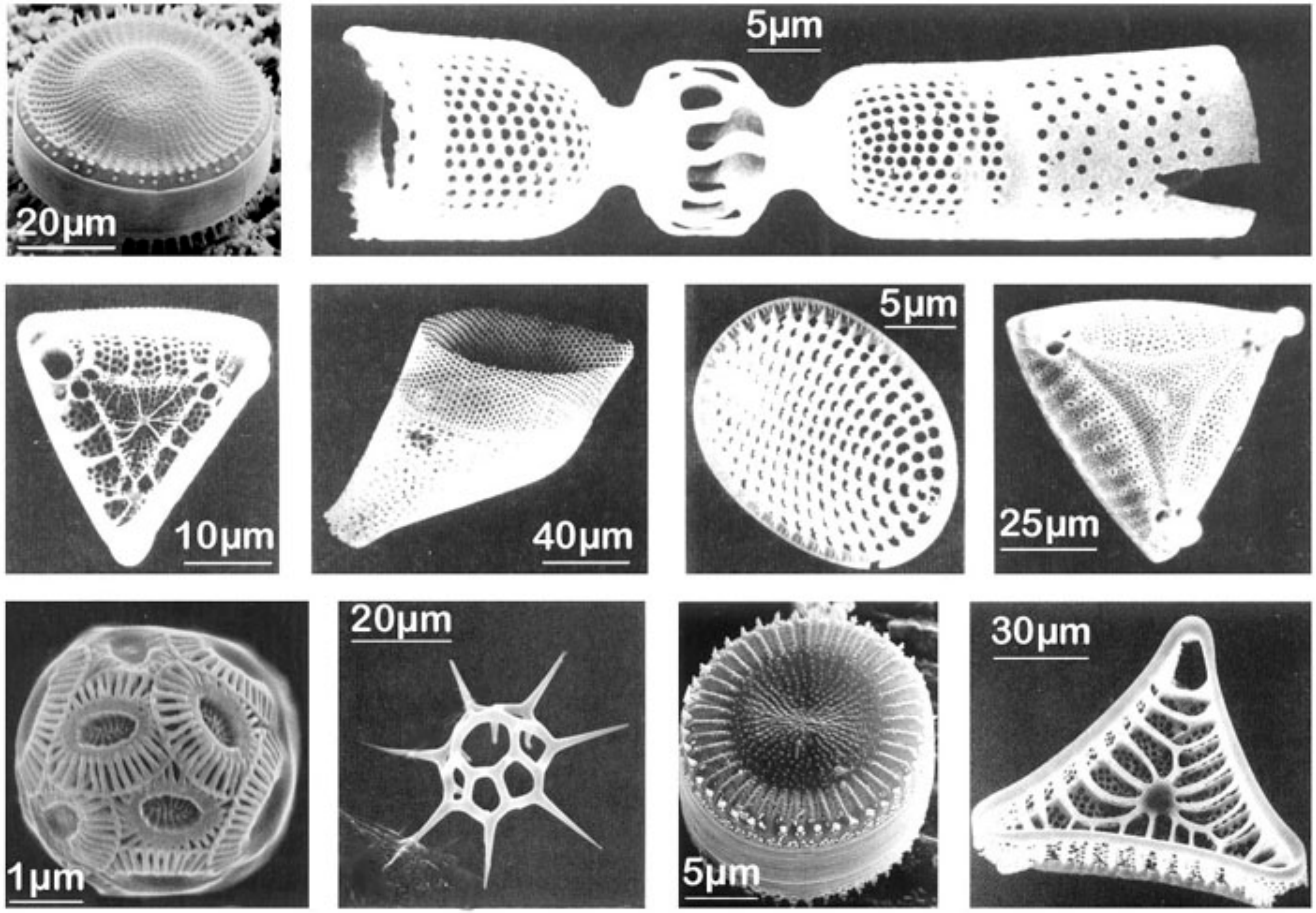

Selection of planktonic diatoms
(not representative for the mediterranian)

dunkel@math.mit.edu

Plants

unlike animal cells, every plant cell is surrounded by a polysaccharide cell wall

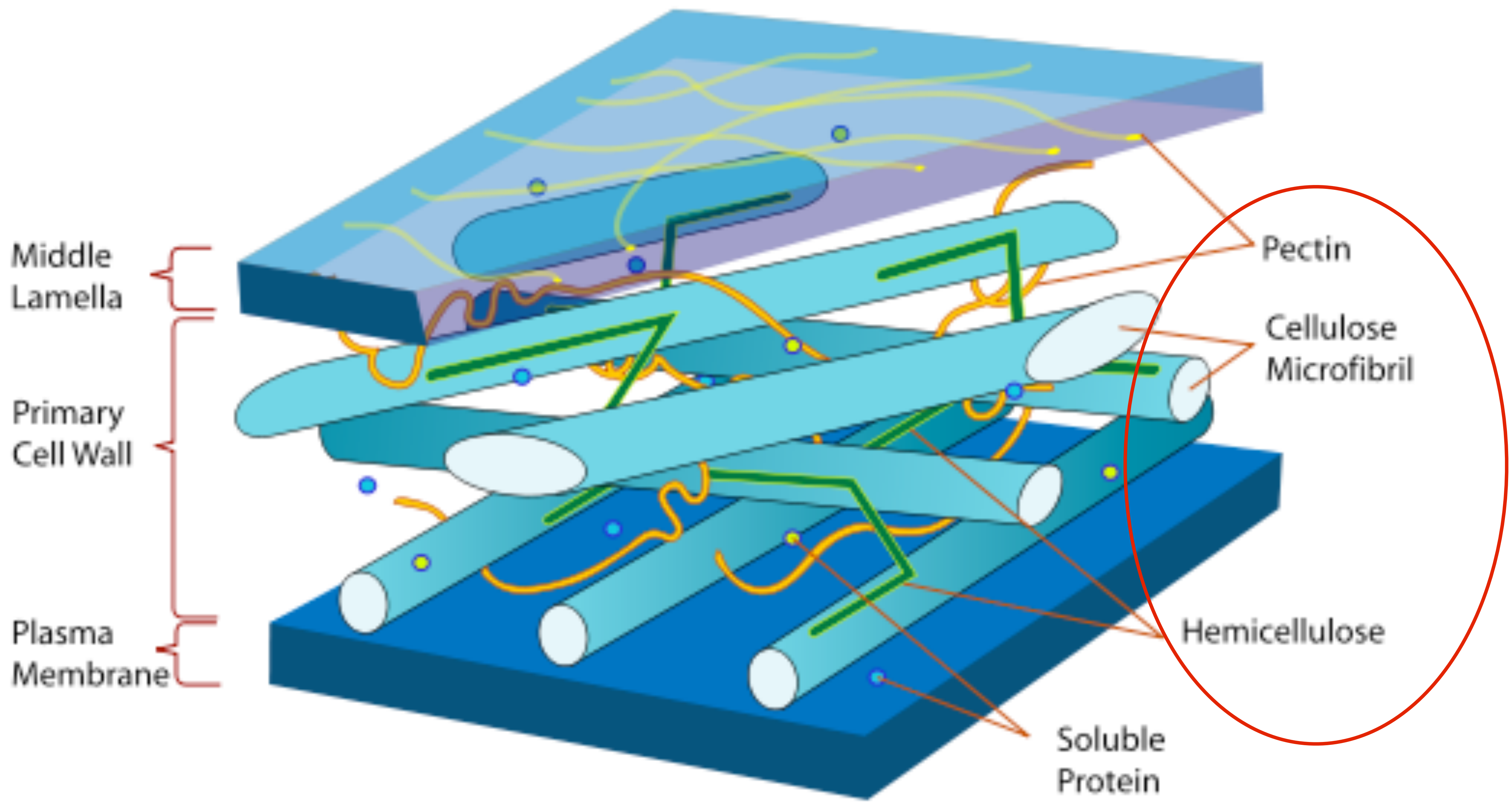

source: wiki

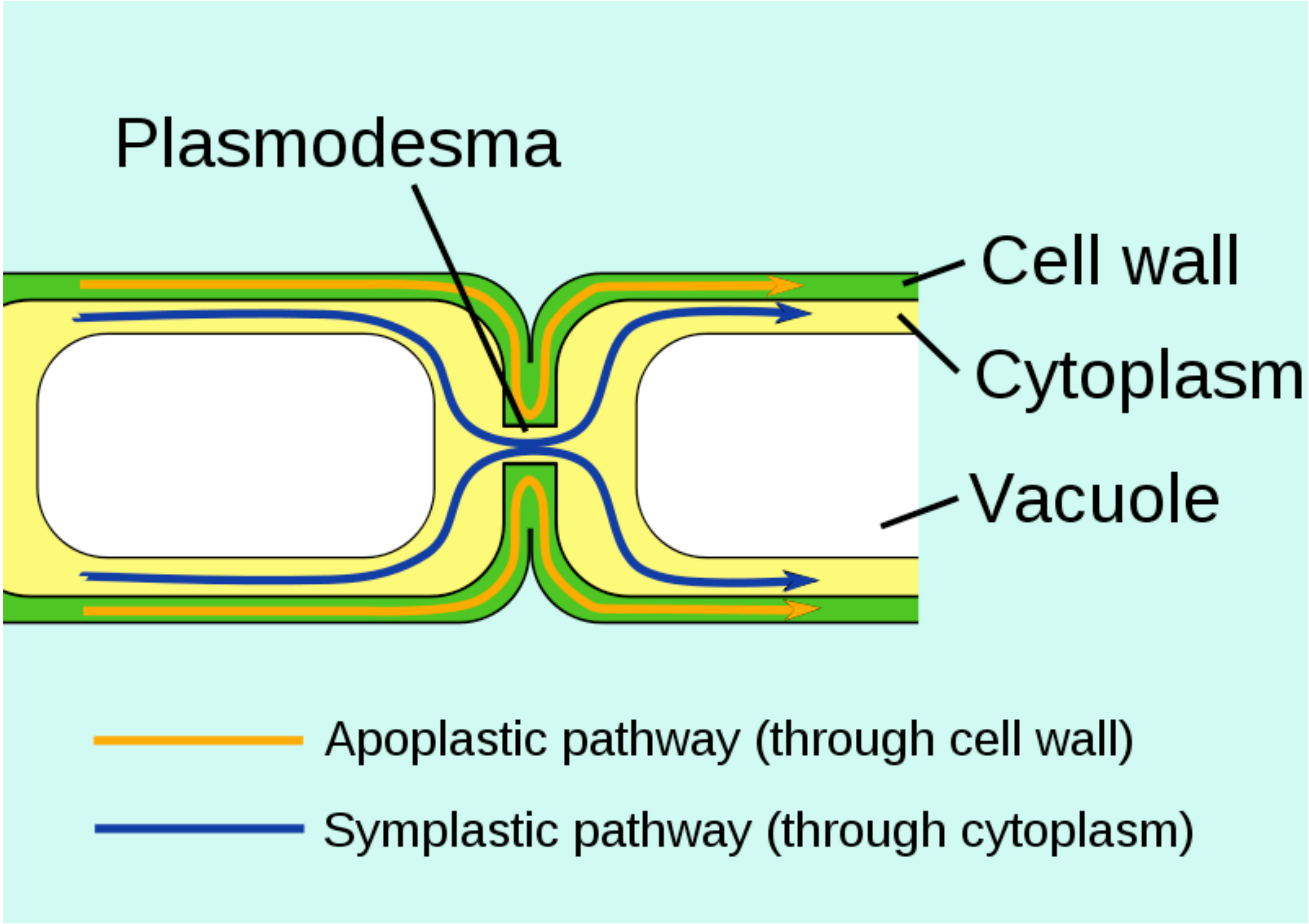

typical plant cell has between 10^3 and 10^5 plasmodesmata
connecting it with adjacent cells
equating to between 1 and 10 per μm

source: wiki

dunkel@math.mit.edu

Chara fragilis

http://www.youtube.com/watch?feature=player_detailpage&v=kud4qUhsCxg

dunkel@math.mit.edu

Characean algae

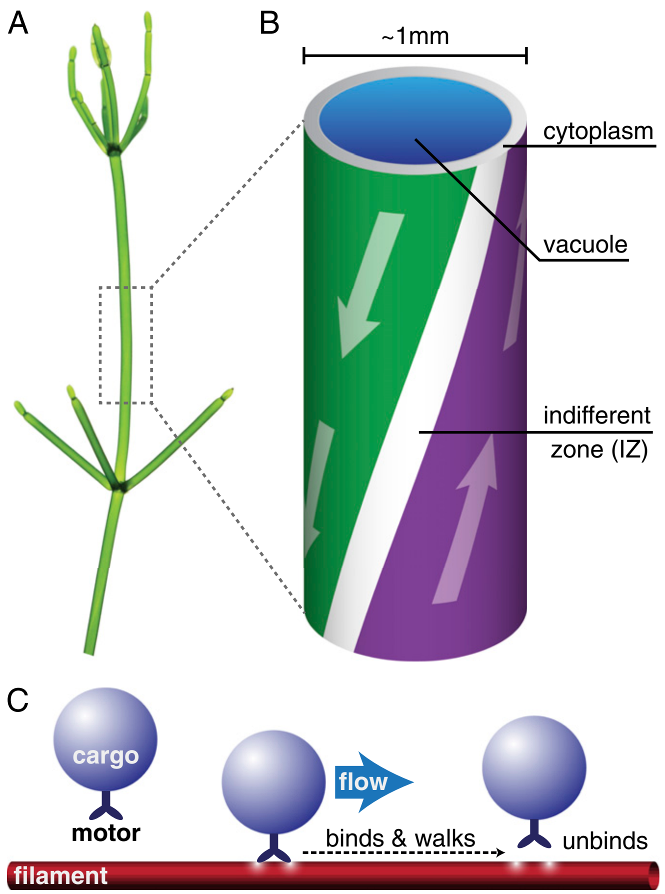

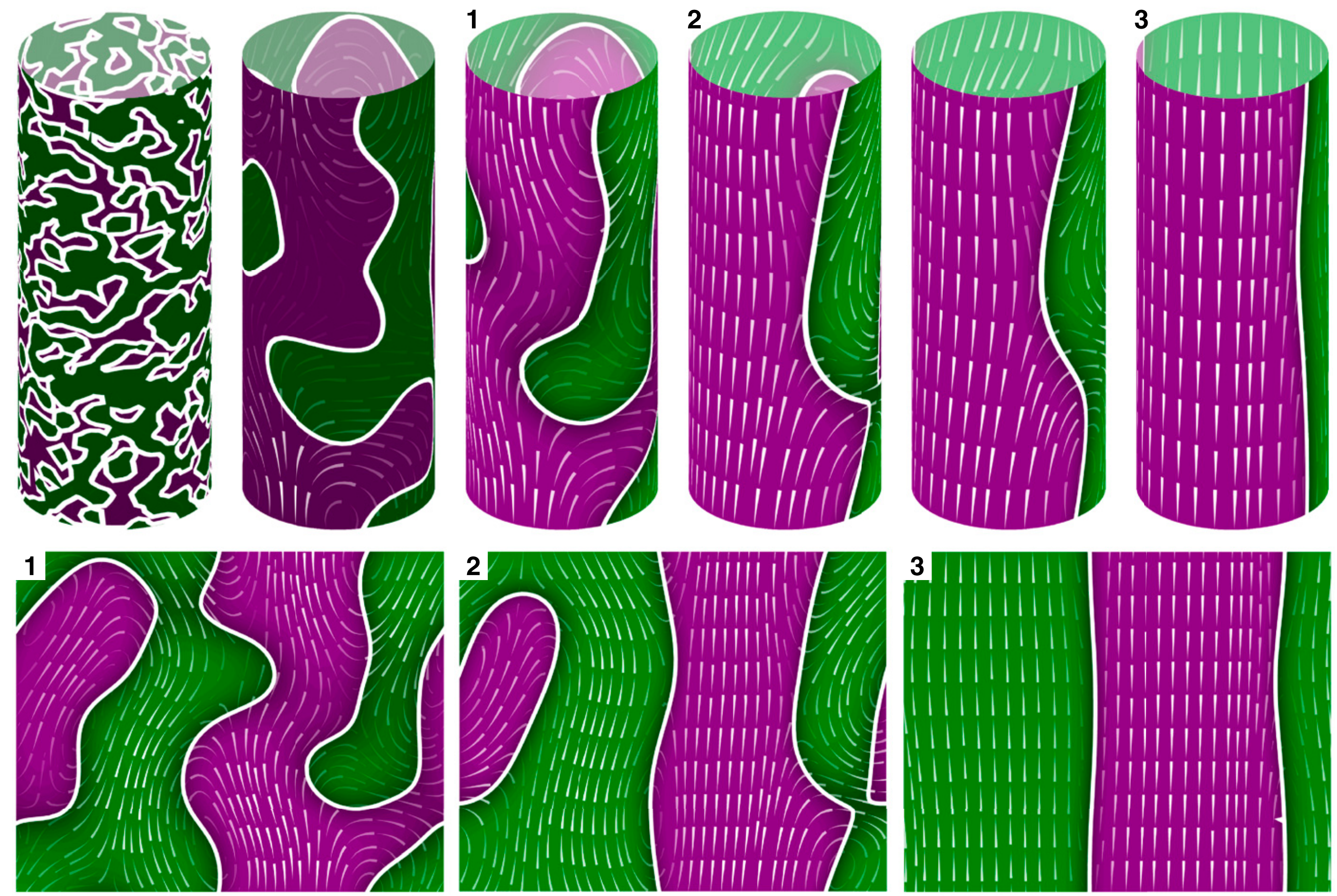

$$-\mu\nabla^2\mathbf{u}+\mathbf{u}+\Pi_0\mathbf{e}_z+\nabla\Pi'=|\mathbf{P}|^2\,\mathbf{P},$$

$$\nabla\cdot\mathbf{u}=0$$

$$\frac{\partial\mathbf{P}}{\partial t}+\epsilon\mathbf{u}\cdot\nabla\mathbf{P}=d^{(s)}\nabla^2\mathbf{P}-d^{(r)}\mathbf{P}+(\mathbb{I}-\mathbf{PP})\cdot[\epsilon(\nabla\mathbf{u})\cdot\mathbf{P}$$
$$+\alpha_p\mathbf{P}+\alpha_u\mathbf{u}-\kappa(\mathbf{P}\cdot\mathbf{d})\mathbf{d}],$$

Woodhouse & Goldstein (2013) PNAS

dunkel@math.mit.edu

Blood cells: shape & function

source: wiki

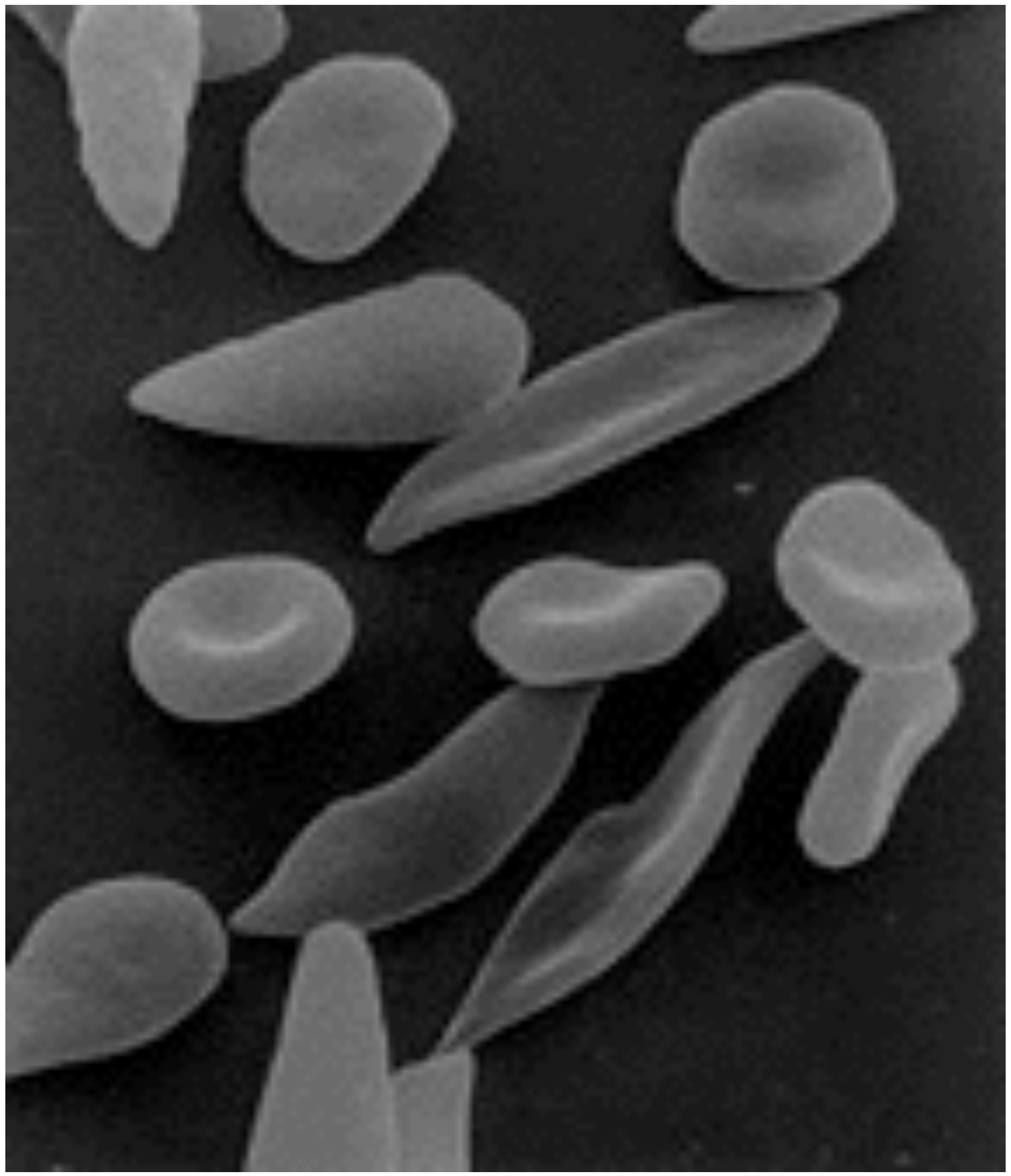

red blood cells affected by sickle-cell disease

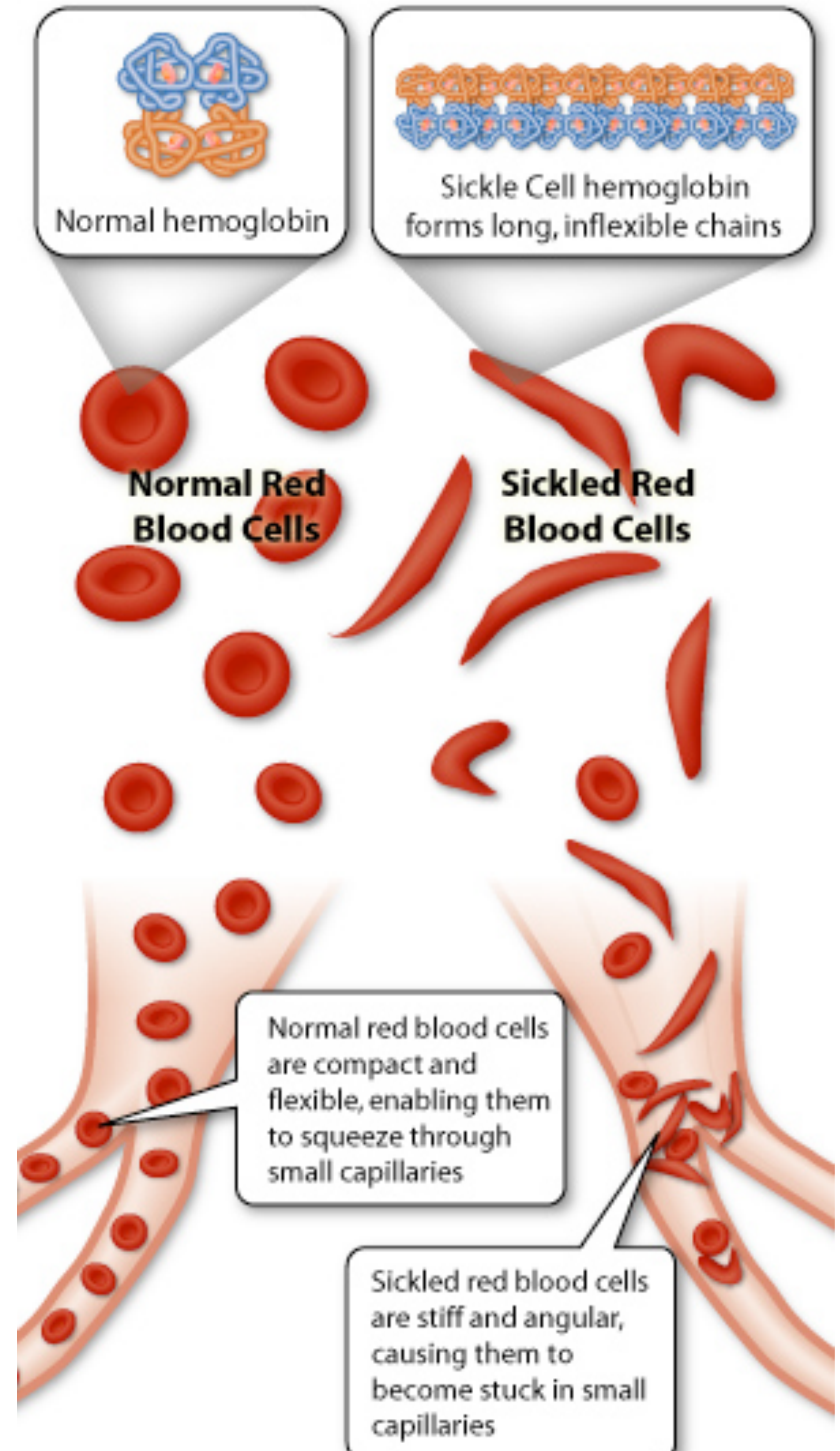

http://learn.genetics.utah.edu/

dunkel@math.mit.edu

Optical tweezer

source: wiki

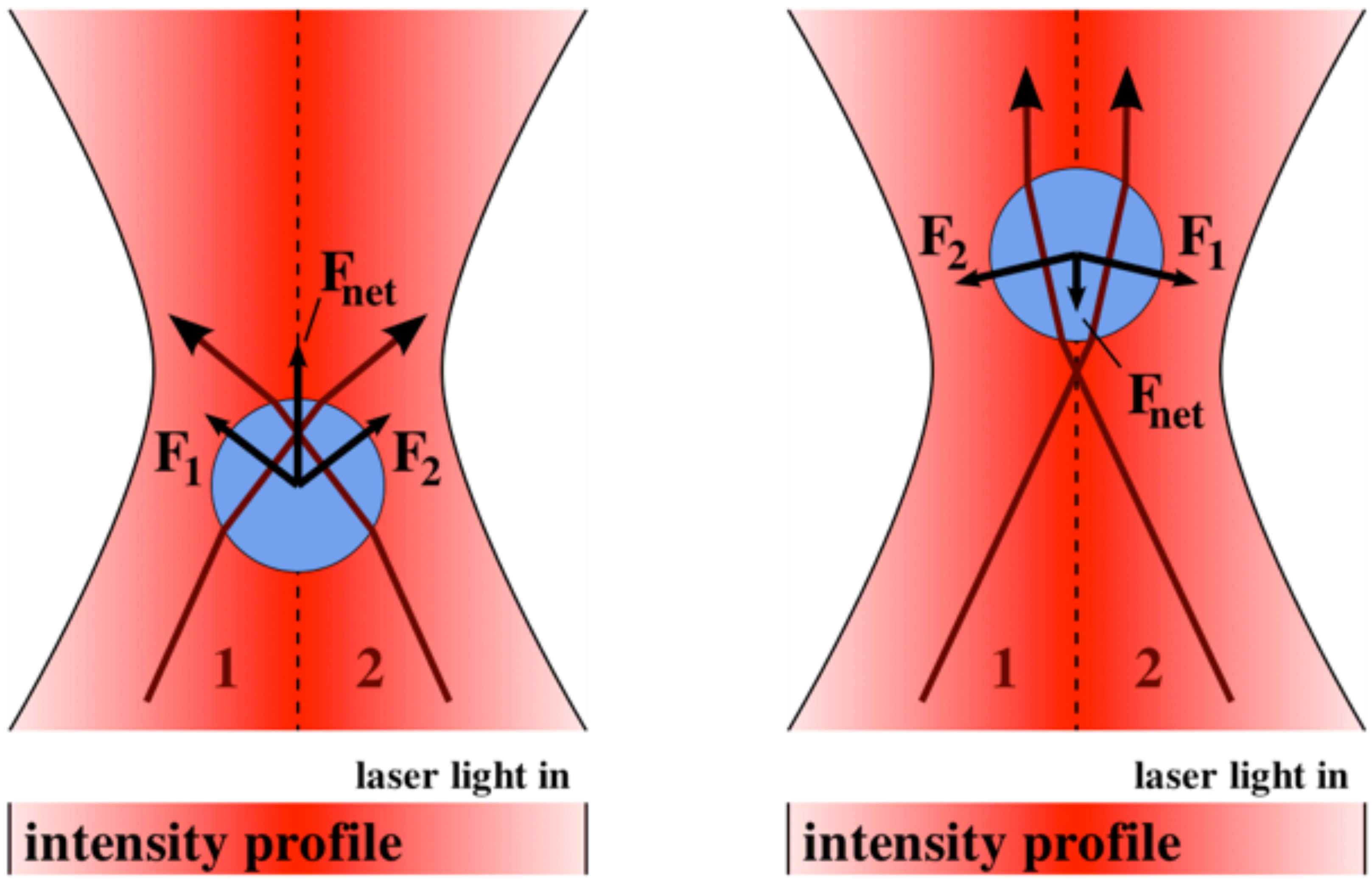

http://www.nature.com/ncomms/journal/v4/n4/extref/ncomms2786-s1.swf

dunkel@math.mit.edu

Red blood cell in tweezer

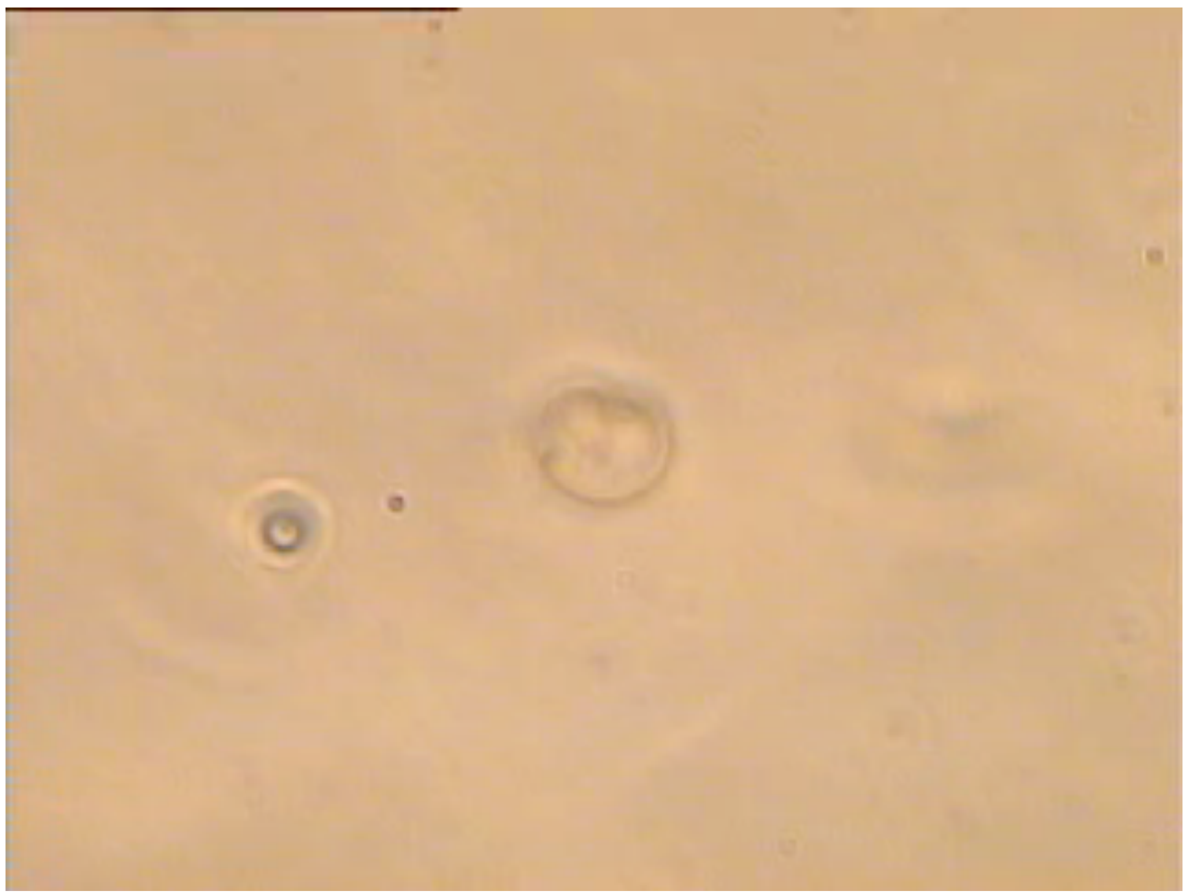

Basu et al (2011) Biophys J

dunkel@math.mit.edu

Full dynamics of a red blood cell in shear flow

Jules Dupire, Marius Socol, and Annie Viallat[1]

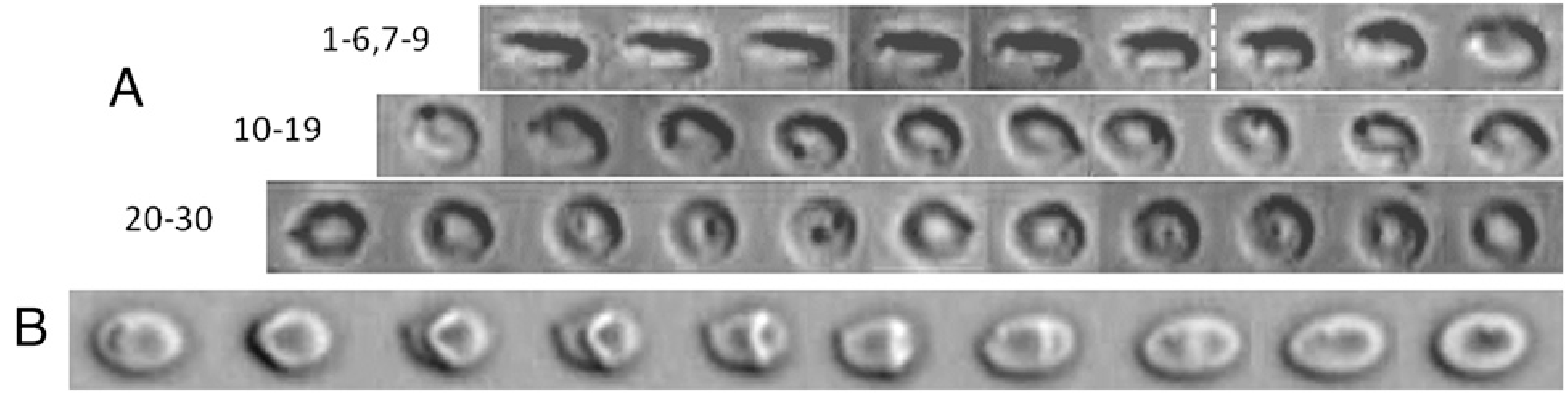

Fig. 5. Rolling-to-tank-treading transition observed on RBCs bearing a bead; dextran 2 10^6 g/mol, c = 9% (wt/wt); scale bar, 8 μm; top-view observation. (*A*) Shear rate = 3 s^{-1}. The symmetry axis of the rolling cell (images 1–7) rotates gradually (images 8–10). The spinning about the symmetry axis is detected by the bead motion (images 10–19). Finally, the streamlines change and the cell tank-treads (images 20–30). A vertical bar separates the different movements. Sequence of 46.6 s; scale bar, 7 μm. (*B*) The tank-treading movement at the transition sometimes presents an overall rotation of part of the membrane, which behaves locally like a solid by rotating as a whole. $\dot{\gamma} = 6\ s^{-1}$, time sequence of 1.98 s.

PNAS 2012

Full dynamics of a red blood cell in shear flow

Jules Dupire, Marius Socol, and Annie Viallat[1]

Blood cell - simulations

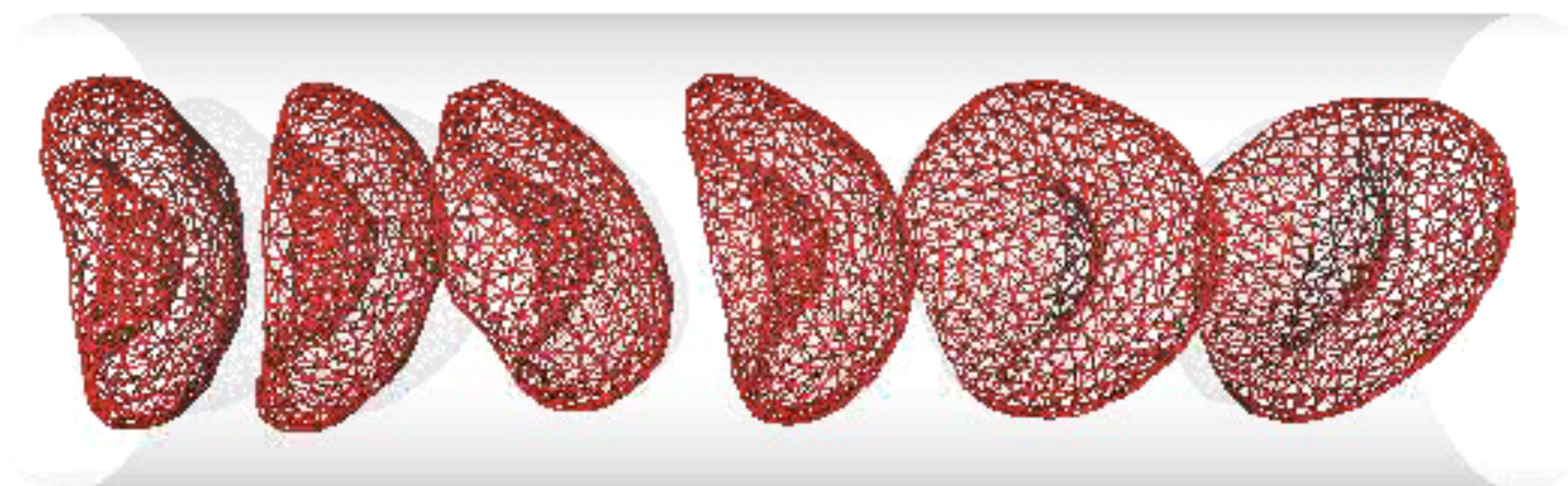

McWhirter et al (2012) New J Phys

Vesicles ("artificial" cells)

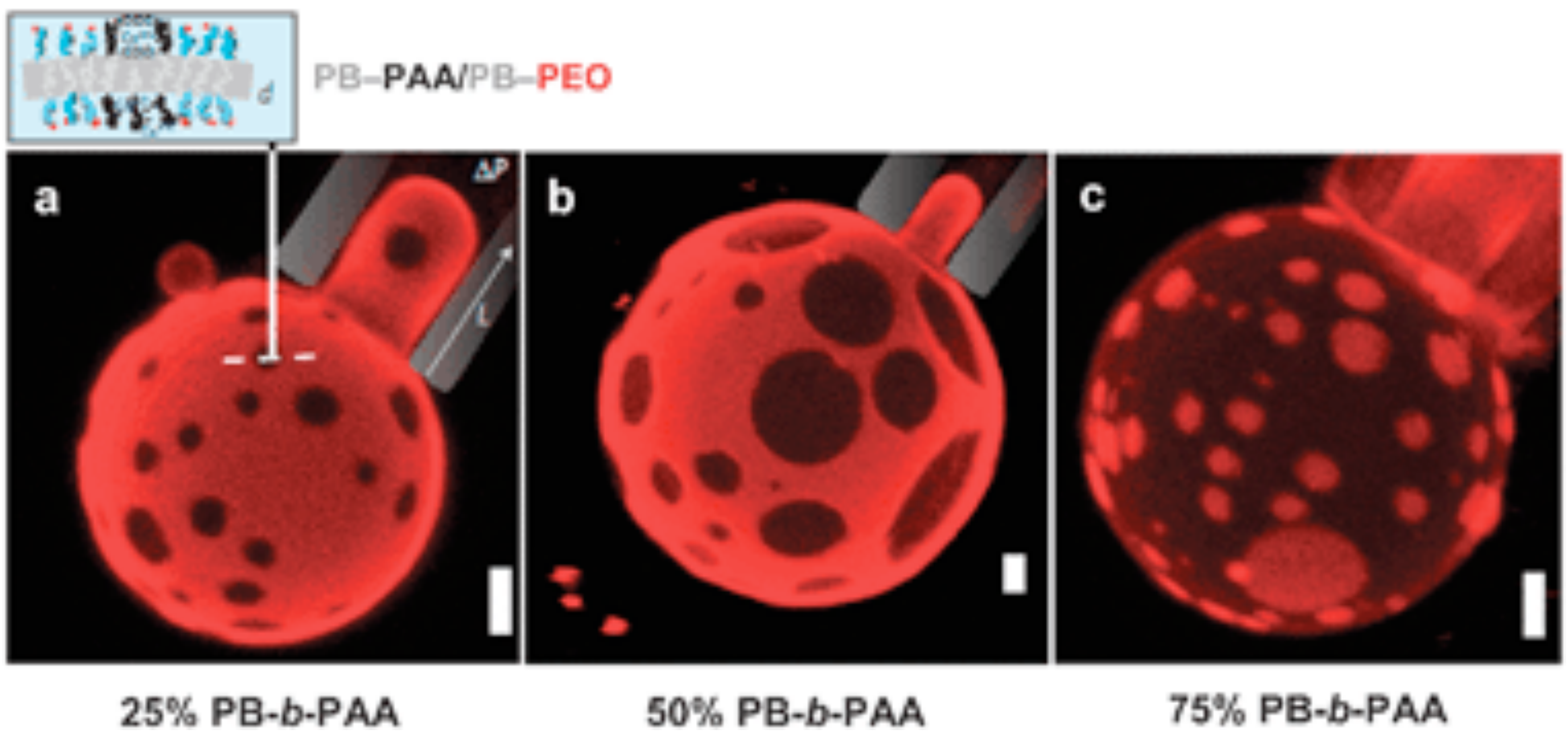

Mai & Eisenberg
Chem Soc Rev 2012

Membrane Viscosity Determined from Shear-Driven Flow in Giant Vesicles

Aurelia R. Honerkamp-Smith, Francis G. Woodhouse, Vasily Kantsler, and Raymond E. Goldstein
Department of Applied Mathematics and Theoretical Physics, Centre for Mathematical Sciences, University of Cambridge, Wilberforce Road, Cambridge CB3 0WA, United Kingdom
(Received 14 January 2013; published 17 July 2013)

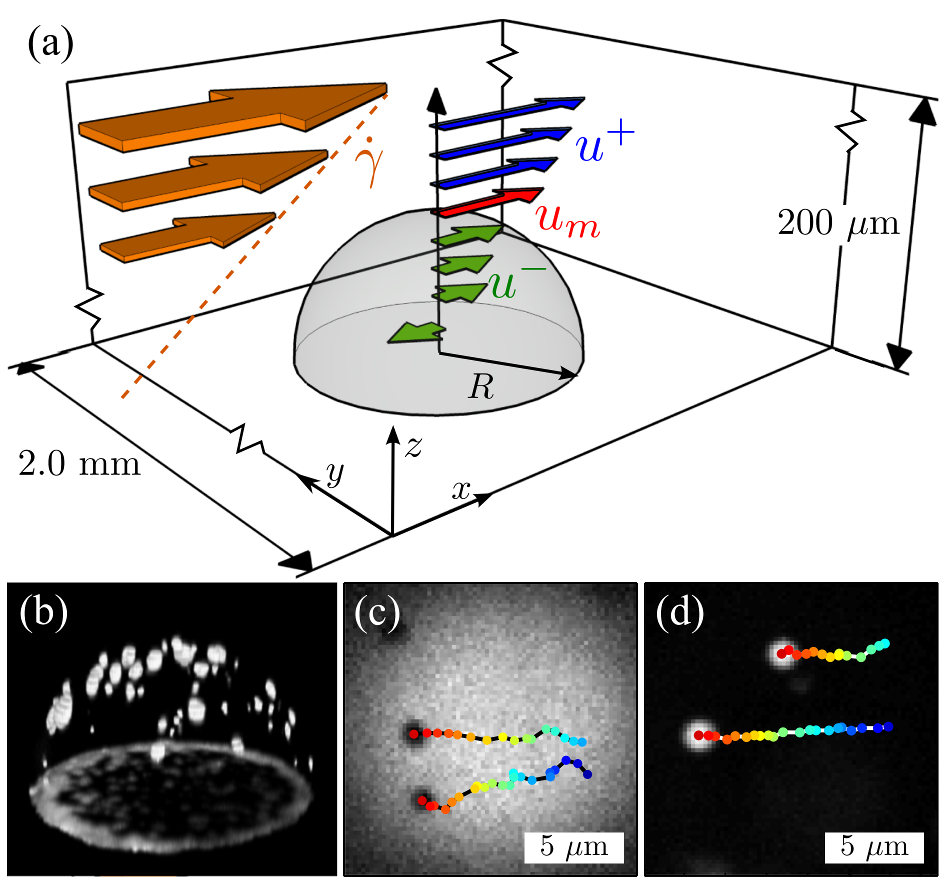

FIG. 1 (color online). Microfluidic shear experiment. (a) Schematic of the chamber (not to scale) and flows. (b) Confocal imaging reconstruction of an adhering hemispherical L_o phase vesicle with small L_d domains visible on its surface. (c)–(d) Tracking of gel domains in L_d background (c) and L_d domains in L_o background (d), flowing across the vesicle apex at $\dot{\gamma} = 2.6\ \mathrm{s}^{-1}$ (tracks color-coded in time over ~2.6 s).

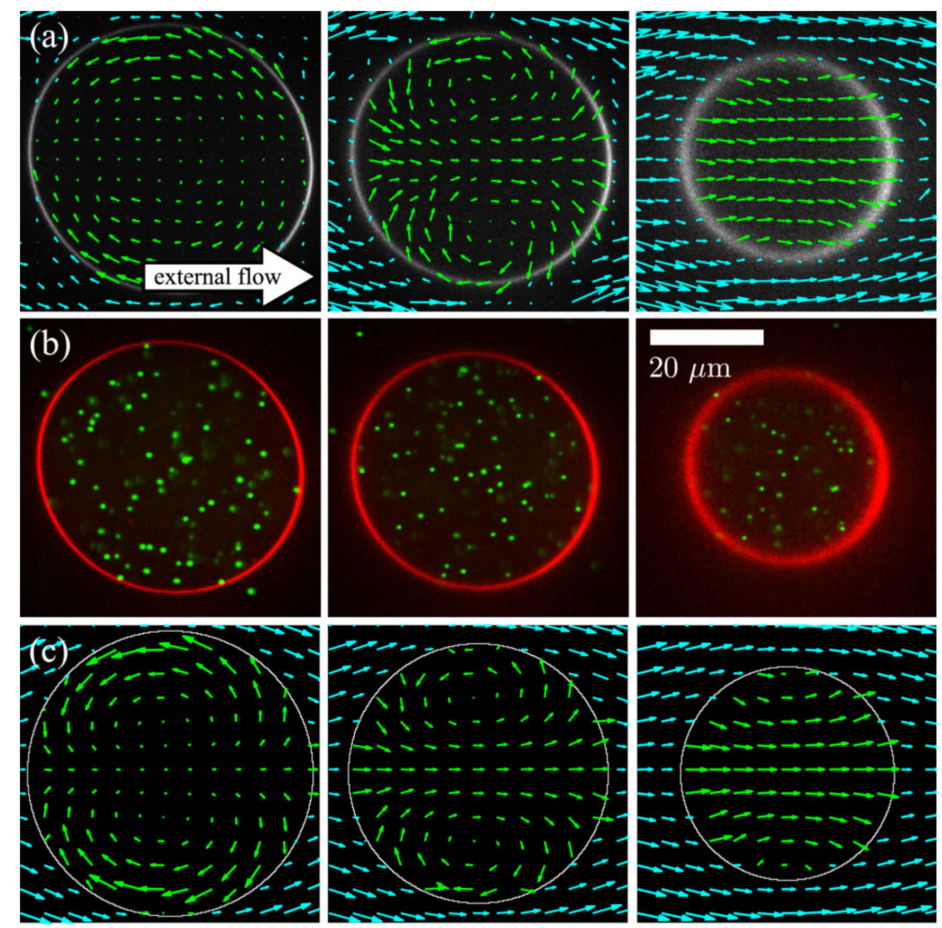

FIG. 2 (color online). Flow fields inside an adhering vesicle in shear. (a) Experimental two-dimensional PIV velocity fields at heights $z/R = 0.26$, 0.47, 0.71 above coverslip. (b) Confocal slices at same fractional heights as (a) show vesicle (red) containing fluorescent microspheres. (c) Theoretical two-dimensional velocity fields [25] for a sheared hemispherical vesicle at $z/R = 0.3$, 0.5, 0.7. Interior and exterior PIV vectors

Membrane Viscosity Determined from Shear-Driven Flow in Giant Vesicles

Aurelia R. Honerkamp-Smith, Francis G. Woodhouse, Vasily Kantsler, and Raymond E. Goldstein
Department of Applied Mathematics and Theoretical Physics, Centre for Mathematical Sciences, University of Cambridge, Wilberforce Road, Cambridge CB3 0WA, United Kingdom
(Received 14 January 2013; published 17 July 2013)

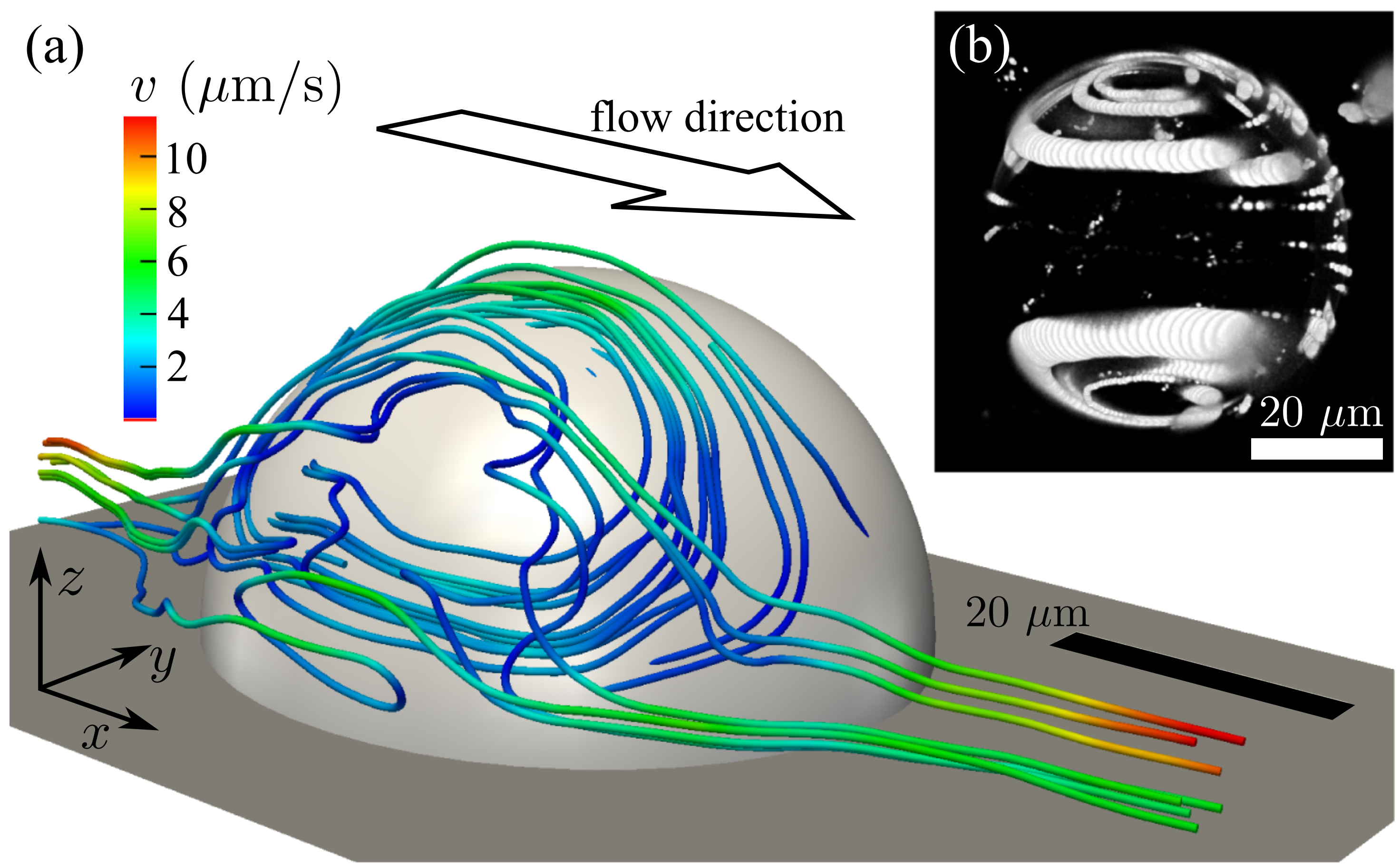

FIG. 3 (color online). Membrane and external flows. (a) Selected external streamlines along one side of an L_o vesicle in shear flow, showing closed orbits above the surface. (b) Time-lapse confocal stack of an L_o vesicle, viewed from above, illustrating circulation of L_d domains.

Membrane Viscosity Determined from Shear-Driven Flow in Giant Vesicles

Aurelia R. Honerkamp-Smith, Francis G. Woodhouse, Vasily Kantsler, and Raymond E. Goldstein
Department of Applied Mathematics and Theoretical Physics, Centre for Mathematical Sciences, University of Cambridge, Wilberforce Road, Cambridge CB3 0WA, United Kingdom
(Received 14 January 2013; published 17 July 2013)

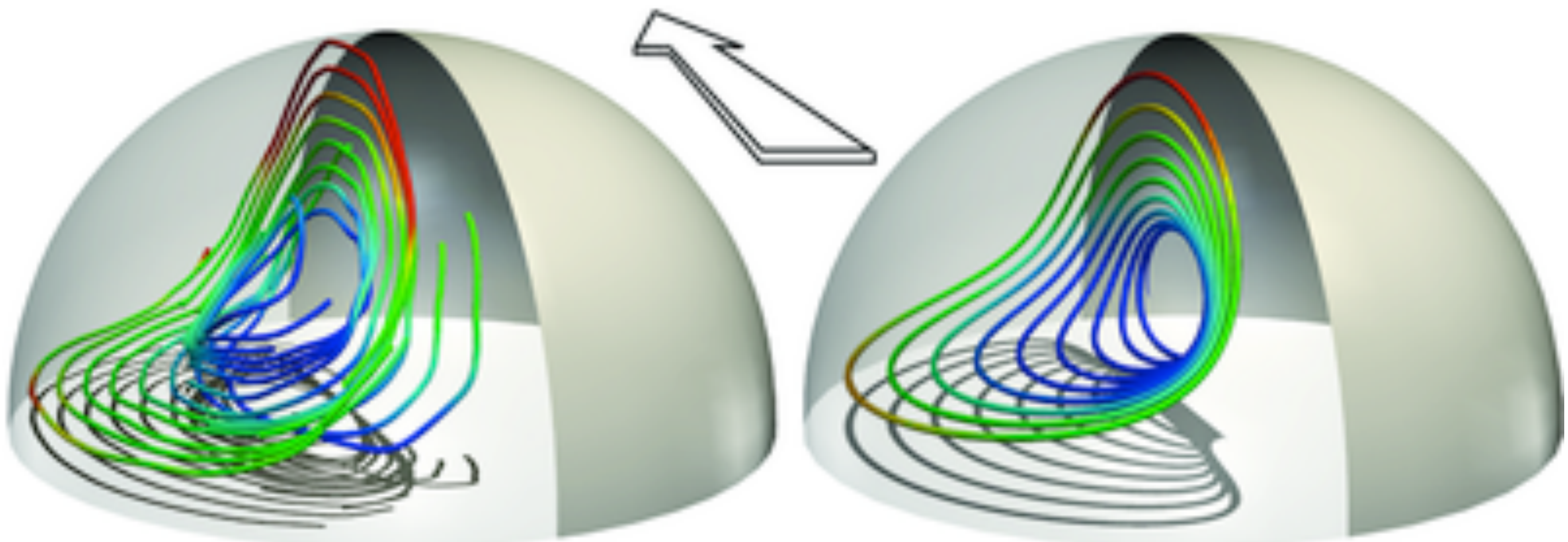

dunkel@math.mit.edu

Dynamics of a vesicle in general flow

J. Deschamps, V. Kantsler, E. Segre, and V. Steinberg[1]

Department of Physics of Complex Systems, Weizmann Institute of Science, Rehovot, 76100 Israel

11444–11447 | PNAS | July 14, 2009 | vol. 106 | no. 28

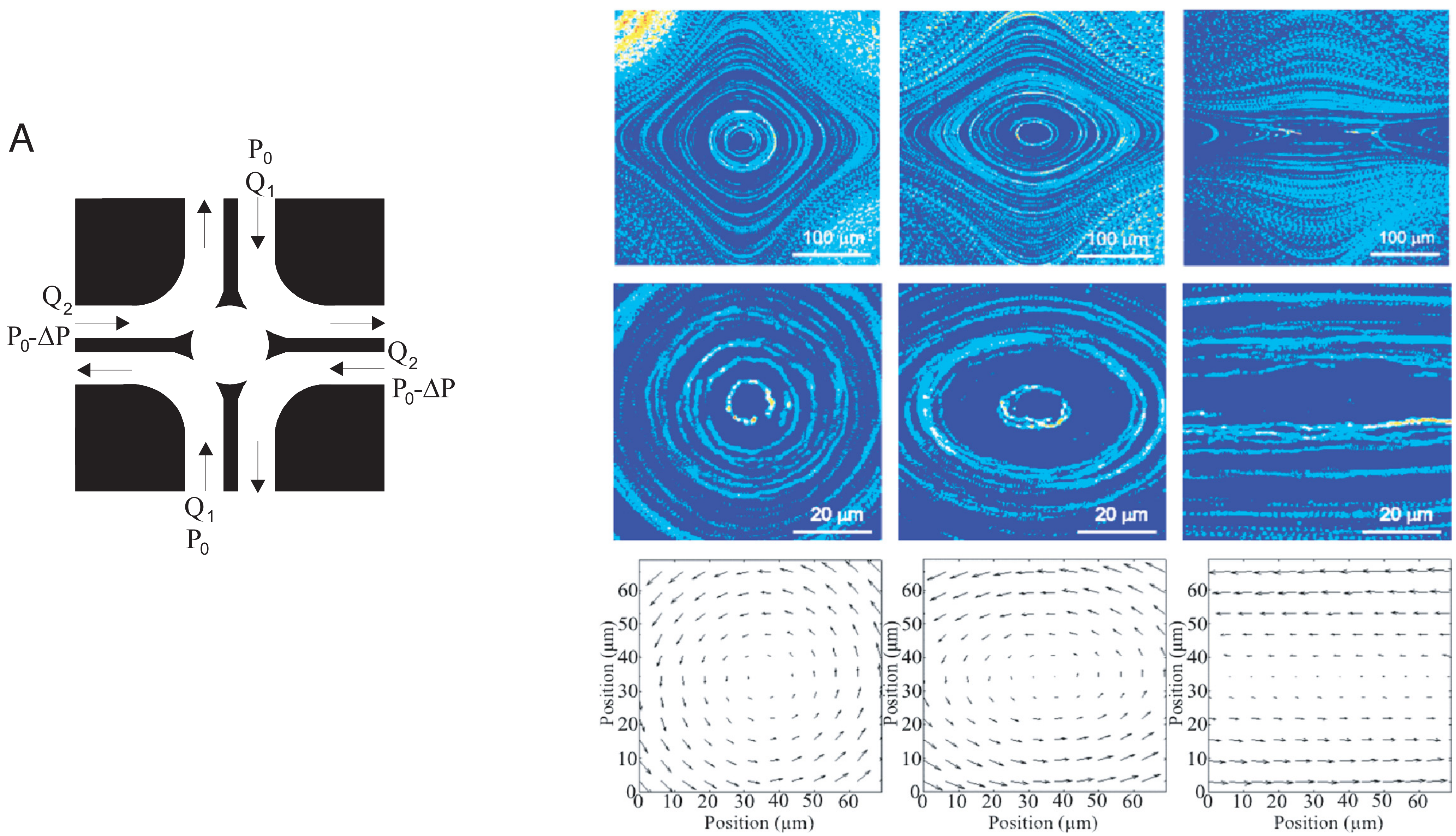

Fig. 2. (*A*) Experimental streamlines images of the velocity fields for pure rotational (first column, $\omega/s = 43$), mixed (second column, $\omega/s = 2.6$) and pure shear (third, $\omega/s = 1$) flows; (*B*) Zoom of the same experimental flows; (*C*) velocity vector field representation of the same flows (PTV).

dunkel@math.mit.edu

PNAS

Dynamics of a vesicle in general flow

J. Deschamps, V. Kantsler, E. Segre, and V. Steinberg[1]

Department of Physics of Complex Systems, Weizmann Institute of Science, Rehovot, 76100 Israel

11444–11447 | PNAS | **July 14, 2009** | vol. 106 | no. 28

A

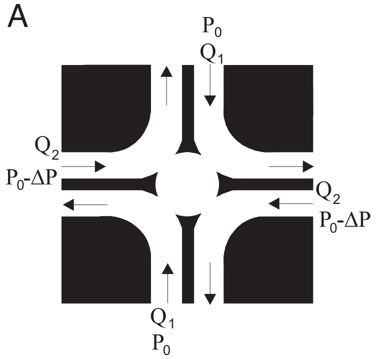

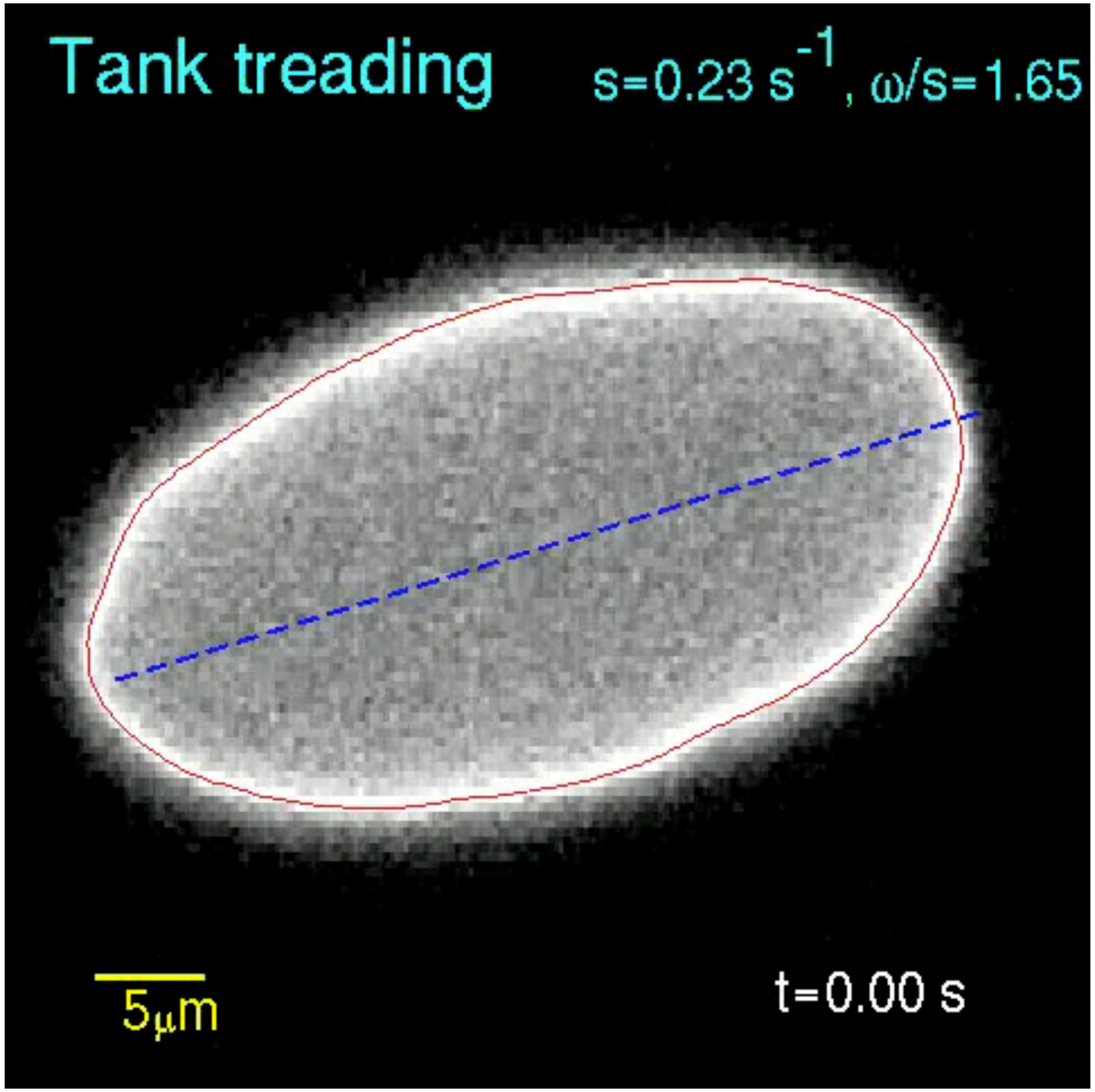

dunkel@math.mit.edu

NATURE | VOL 423 | 8 MAY 2003 | www.nature.com/nature

Controlled vesicle deformation and lysis by single oscillating bubbles

Philippe Marmottant & Sascha Hilgenfeldt

Faculty of Applied Physics, University of Twente, PO Box 217, 7500AE Enschede, The Netherlands

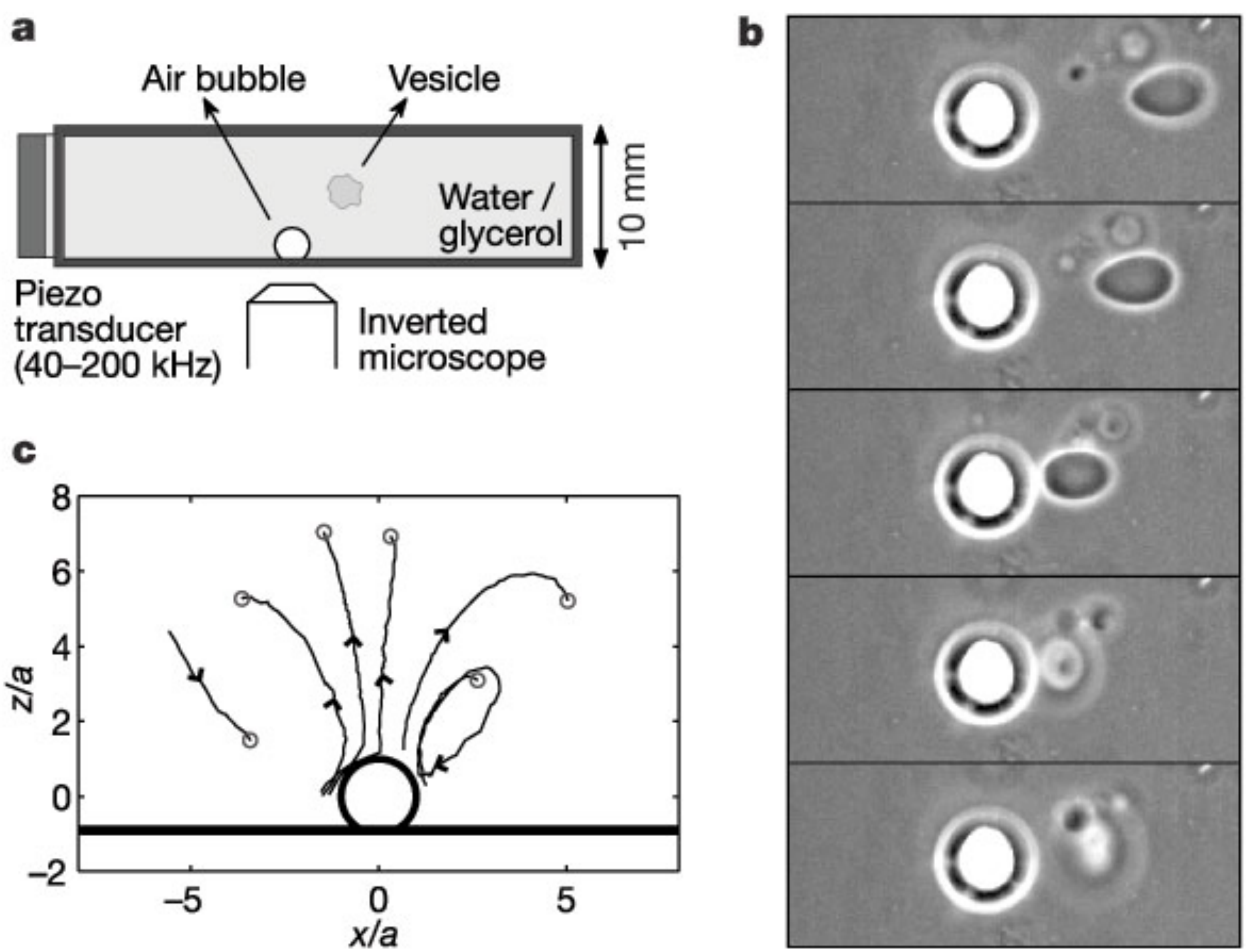

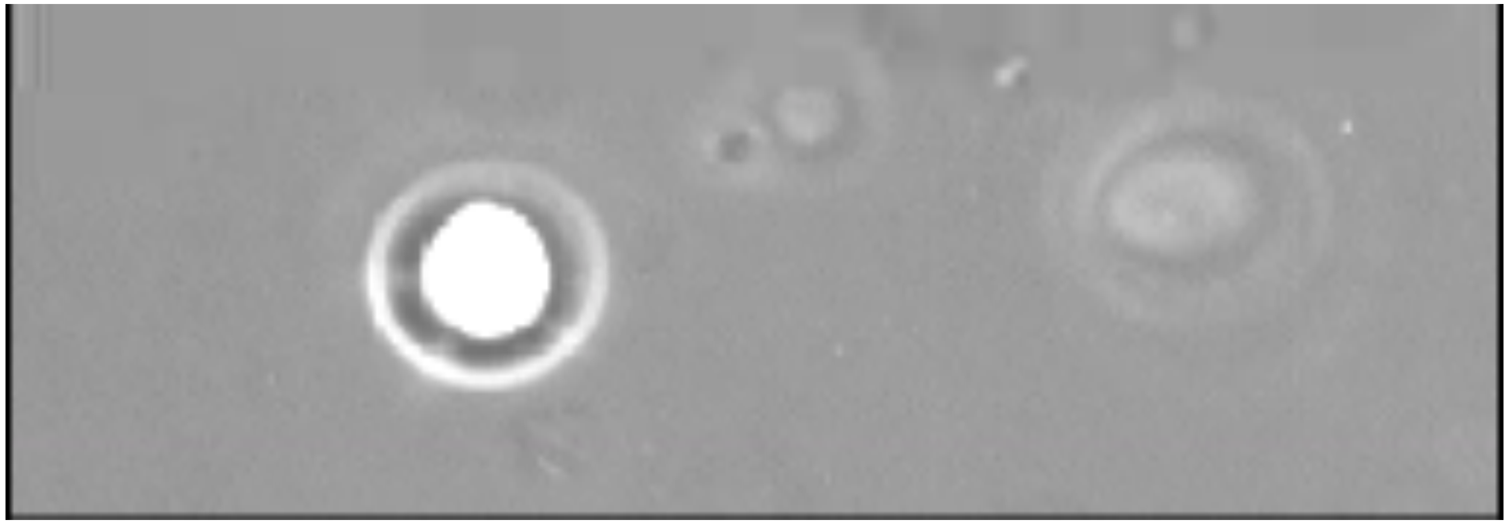

NATURE | VOL 423 | 8 MAY 2003 | www.nature.com/nature

letters to nature

Controlled vesicle deformation and lysis by single oscillating bubbles

Philippe Marmottant & Sascha Hilgenfeldt

Faculty of Applied Physics, University of Twente, PO Box 217, 7500AE Enschede, The Netherlands

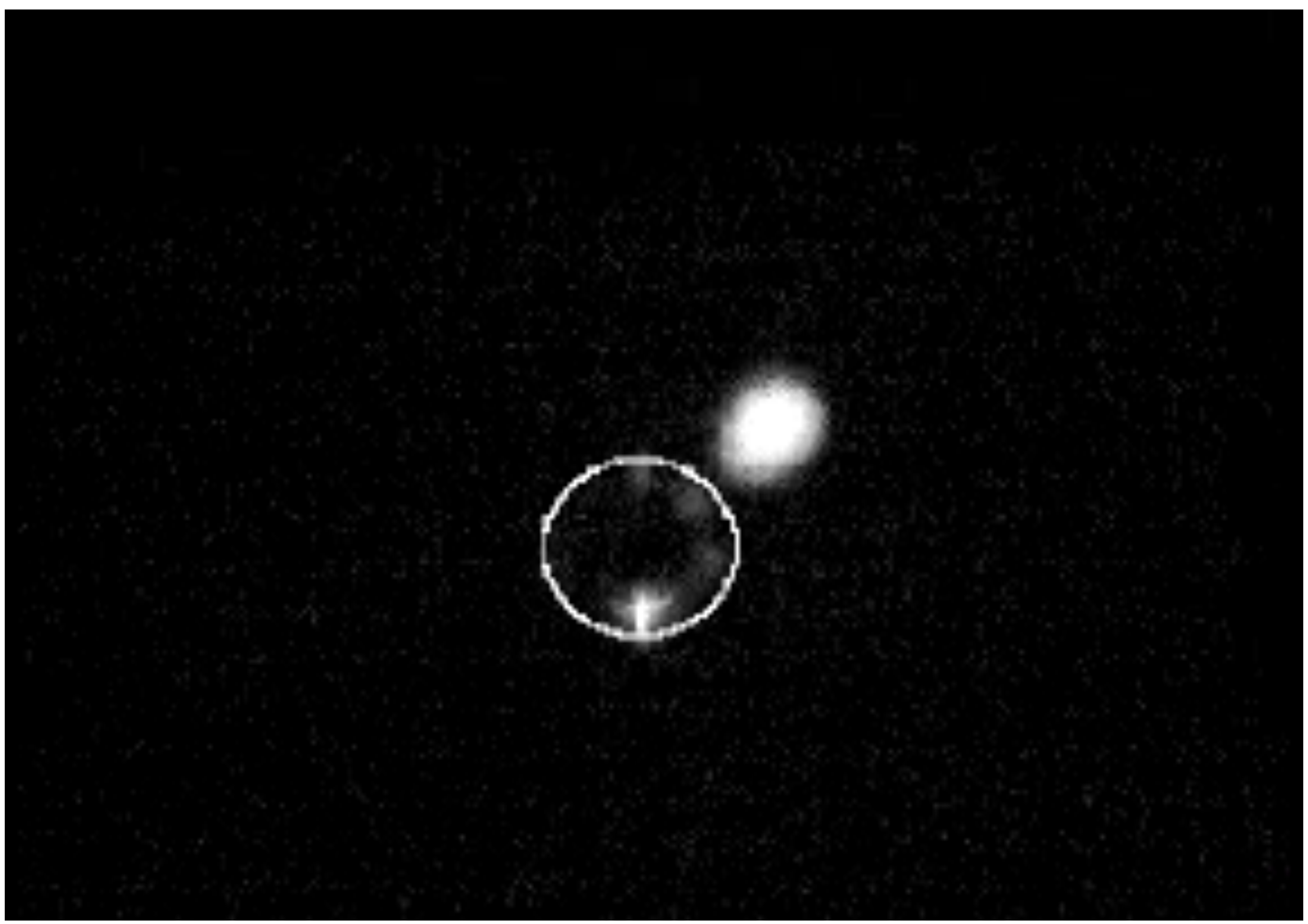

Chapter 3

Membranes

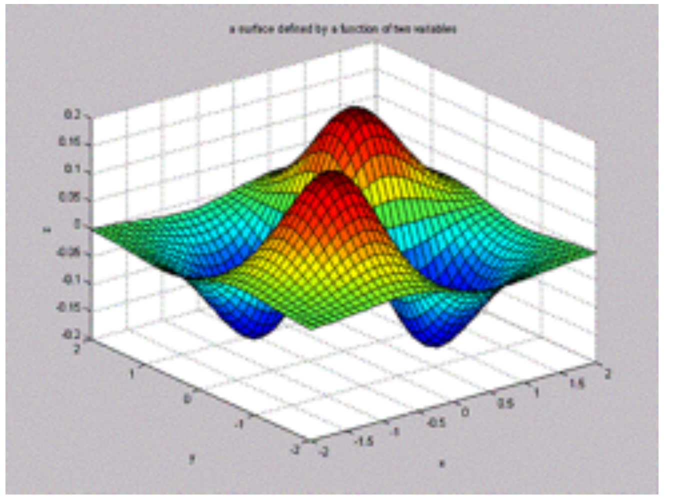

The discussion in this section builds on the review article [Sei97] and the textbook [OLXY99].

3.1 Reminder: 2D differential geometry

We consider an orientable surface in $\mathbb{R}^3$. Possible local parameterizations are

$$\boldsymbol{F}(s_1, s_2) \in \mathbb{R}^3 \tag{3.1}$$

where $(s_1, s_2) \in U \subseteq \mathbb{R}^2$. Alternatively, if one chooses Cartesian coordinates $(s_1, s_2) = (x, y)$, then it suffices to specify

$$z = f(x, y) \tag{3.2a}$$

or, equivalently, the implicit representation

$$\Phi(x, y, z) = z - f(x, y). \tag{3.2b}$$

The vector representation (3.1) can be related to the 'height' representation (3.2a) by

$$\boldsymbol{F}(x, y) = \begin{pmatrix} x \\ y \\ f(x, y) \end{pmatrix} \tag{3.3}$$

dunkel@math.mit.edu

Surface metric tensor

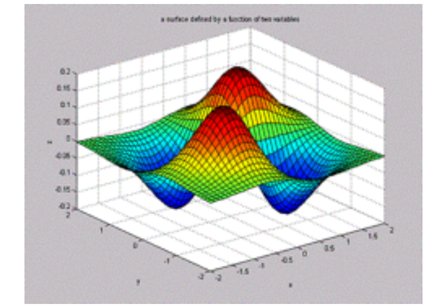

$$\boldsymbol{F}(x,y) = \begin{pmatrix} x \\ y \\ f(x,y) \end{pmatrix} \tag{3.3}$$

Denoting derivatives by $\boldsymbol{F}_i = \partial_{s_i}\boldsymbol{F}$, we introduce the surface metric tensor $g = (g_{ij})$ by

$$g_{ij} = \boldsymbol{F}_i \cdot \boldsymbol{F}_j, \tag{3.4a}$$

abbreviate its determinant by

$$|g| := \det g, \tag{3.4b}$$

and define the associated Laplace-Beltrami operator ∇^2 by

$$\nabla^2 h = \frac{1}{\sqrt{|g|}}\partial_i(g_{ij}^{-1}\sqrt{|g|}\partial_j h), \tag{3.4c}$$

for some function $h(s_1, s_2)$.

dunkel@math.mit.edu

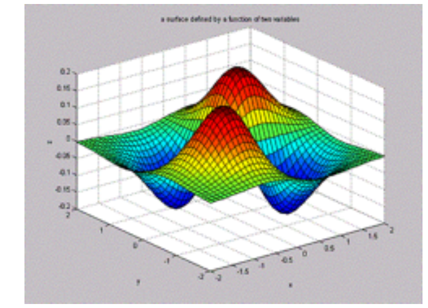

$$\boldsymbol{F}(x,y) = \begin{pmatrix} x \\ y \\ f(x,y) \end{pmatrix} \tag{3.3}$$

Denoting derivatives by $\boldsymbol{F}_i = \partial_{s_i}\boldsymbol{F}$, we introduce the surface metric tensor $g = (g_{ij})$ by

$$g_{ij} = \boldsymbol{F}_i \cdot \boldsymbol{F}_j, \tag{3.4a}$$

abbreviate its determinant by

$$|g| := \det g, \tag{3.4b}$$

$$\boldsymbol{F}_x(x,y) = \begin{pmatrix} 1 \\ 0 \\ f_x \end{pmatrix}, \qquad \boldsymbol{F}_y(x,y) = \begin{pmatrix} 0 \\ 1 \\ f_y \end{pmatrix} \tag{3.5}$$

and, hence, the metric tensor

$$g = (g_{ij}) = \begin{pmatrix} \boldsymbol{F}_x \cdot \boldsymbol{F}_x & \boldsymbol{F}_x \cdot \boldsymbol{F}_y \\ \boldsymbol{F}_y \cdot \boldsymbol{F}_x & \boldsymbol{F}_y \cdot \boldsymbol{F}_y \end{pmatrix} = \begin{pmatrix} 1 + f_x^2 & f_x f_y \\ f_y f_x & 1 + f_y^2 \end{pmatrix} \tag{3.6a}$$

and its determinant

$$|g| = 1 + f_x^2 + f_y^2, \tag{3.6b}$$

where $f_x = \partial_x f$ and $f_y = \partial_y f$. For later use, we still note that the inverse of the metric tensor is given by

$$g^{-1} = (g_{ij}^{-1}) = \frac{1}{1 + f_x^2 + f_y^2} \begin{pmatrix} 1 + f_y^2 & -f_x f_y \\ -f_y f_x & 1 + f_x^2 \end{pmatrix}. \tag{3.6c}$$

dunkel@math.mit.edu

Surface normal & curvature

Assuming the surface is regular at (s_1, s_2), which just means that the tangent vectors $\boldsymbol{F}_1$ and $\boldsymbol{F}_2$ are linearly independent, the local unit normal vector is defined by

$$\boldsymbol{N} = \frac{\boldsymbol{F}_1 \wedge \boldsymbol{F}_2}{||\boldsymbol{F}_1 \wedge \boldsymbol{F}_2||}. \tag{3.7}$$

In terms of the Cartesian parameterization, this can also be rewritten as

$$\boldsymbol{N} = \frac{\nabla\Phi}{||\nabla\Phi||} = \frac{1}{\sqrt{1 + f_x^2 + f_y^2}} \begin{pmatrix} -f_x \\ -f_y \\ 1 \end{pmatrix}. \tag{3.8}$$

Here, we have adopted the convention that $\{\boldsymbol{F}_1, \boldsymbol{F}_2, \boldsymbol{N}\}$ form a right-handed system.

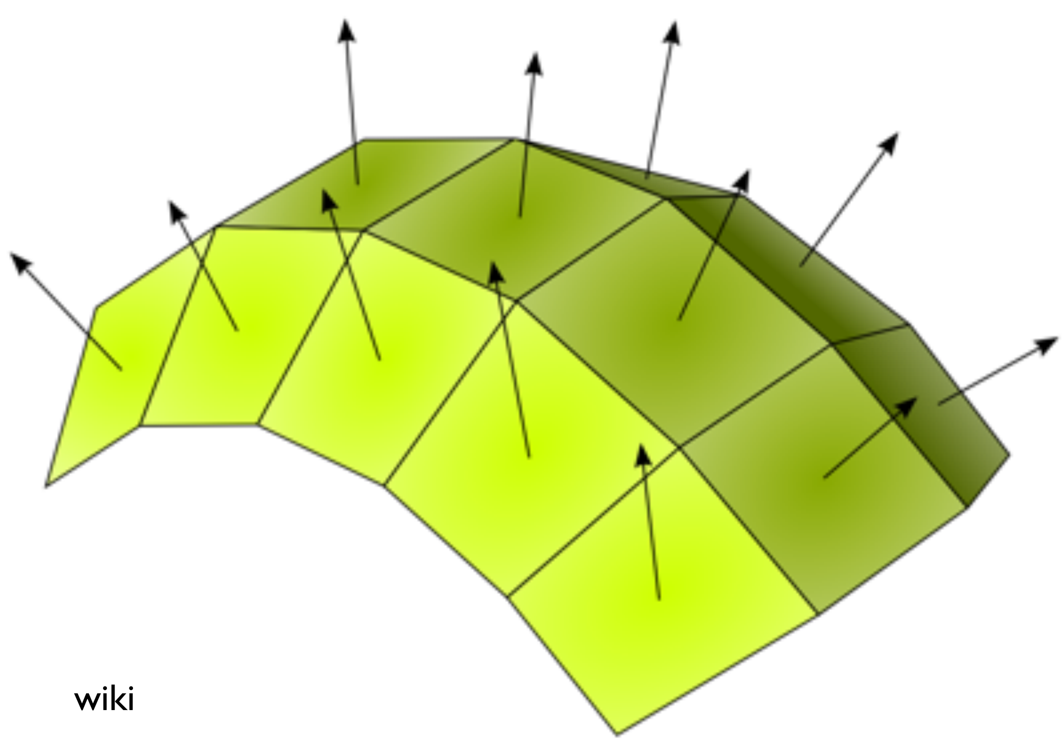

wiki

Surface normal & curvature

Assuming the surface is regular at (s_1, s_2), which just means that the tangent vectors $\boldsymbol{F}_1$ and $\boldsymbol{F}_2$ are linearly independent, the local unit normal vector is defined by

$$\boldsymbol{N} = \frac{\boldsymbol{F}_1 \wedge \boldsymbol{F}_2}{||\boldsymbol{F}_1 \wedge \boldsymbol{F}_2||}. \tag{3.7}$$

In terms of the Cartesian parameterization, this can also be rewritten as

$$\boldsymbol{N} = \frac{\nabla\Phi}{||\nabla\Phi||} = \frac{1}{\sqrt{1 + f_x^2 + f_y^2}} \begin{pmatrix} -f_x \\ -f_y \\ 1 \end{pmatrix}. \tag{3.8}$$

Here, we have adopted the convention that $\{\boldsymbol{F}_1, \boldsymbol{F}_2, \boldsymbol{N}\}$ form a right-handed system.

To formulate 'geometric' energy functionals for membranes, we still require the concept of curvature, which quantifies the local bending of the membrane. We define a 2×2-curvature tensor $R = (R_{ij})$ by

$$R_{ij} = \boldsymbol{N} \cdot (\boldsymbol{F}_{ij}) \tag{3.9}$$

and local *mean curvature* H and local *Gauss curvature* K by

$$H = \frac{1}{2} \mathrm{tr}\left(g^{-1} \cdot R\right), \qquad K = \det(g^{-1} \cdot R). \tag{3.10}$$

Adopting the Cartesian representation (3.2a), we have

$$\boldsymbol{F}_{xx} = \begin{pmatrix} 0 \\ 0 \\ f_{xx} \end{pmatrix}, \qquad \boldsymbol{F}_{xy} = \boldsymbol{F}_{yx} = \begin{pmatrix} 0 \\ 0 \\ f_{xy} \end{pmatrix}, \qquad \boldsymbol{F}_{yy} = \begin{pmatrix} 0 \\ 0 \\ f_{yy} \end{pmatrix} \tag{3.11a}$$

dunkel@math.mit.edu

Surface normal & curvature

yielding the curvature tensor

$$(R_{ij}) = \begin{pmatrix} \boldsymbol{N} \cdot \boldsymbol{F}_{xx} & \boldsymbol{N} \cdot \boldsymbol{F}_{xy} \\ \boldsymbol{N} \cdot \boldsymbol{F}_{yx} & \boldsymbol{N} \cdot \boldsymbol{F}_{yy} \end{pmatrix} = \frac{1}{\sqrt{1 + f_x^2 + f_y^2}} \begin{pmatrix} f_{xx} & f_{xy} \\ f_{yx} & f_{yy} \end{pmatrix} \tag{3.11b}$$

Denoting the eigenvalues of the matrix $g^{-1} \cdot R$ by κ_1 and κ_2, we obtain for the mean curvature

$$H = \frac{1}{2} (\kappa_1 + \kappa_2) = \frac{(1 + f_y^2) f_{xx} - 2 f_x f_y f_{xy} + (1 + f_x^2) f_{yy}}{2(1 + f_x^2 + f_y^2)^{3/2}} \tag{3.12}$$

and for the Gauss curvature

$$K = \kappa_1 \cdot \kappa_2 = \frac{f_{xx} f_{yy} - f_{xy}^2}{(1 + f_x^2 + f_y^2)^2}. \tag{3.13}$$

dunkel@math.mit.edu

Gauss-Bonet Theorem

$$\int_M K\, dA + \oint_{\partial M} k_g\, ds = 2\pi\, \chi(M). \qquad (3.14)$$

Gauss curvature | geodesic curvature | Euler characteristic

$\chi(M) = 2 - 2g$, where g is the *genus*

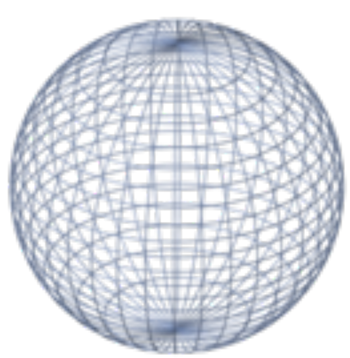

2

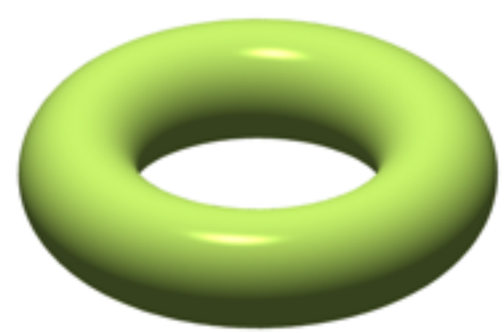

0

-2

wiki

dunkel@math.mit.edu

Gauss-Bonet Theorem

$$\int_M K \, dA + \oint_{\partial M} k_g \, ds = 2\pi \, \chi(M). \tag{3.14}$$

Convex polyhedra

Name	Image	Vertices *V*	Edges *E*	Faces *F*	Euler characteristic: *V* − *E* + *F*
Tetrahedron		4	6	4	**2**
Hexahedron or cube	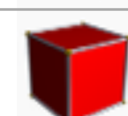	8	12	6	**2**
Octahedron		6	12	8	**2**
Dodecahedron		20	30	12	**2**
Icosahedron		12	30	20	**2**

wiki

dunkel@math.mit.edu

3.2 Minimal surfaces

Minimal surfaces are surfaces that minimize the area within a given contour ∂M,

$$A(M|\partial M) = \int_M dA = \min! \tag{3.15}$$

Assuming a Cartesian parameterization $z = f(x, y)$ and abbreviating $f_i = \partial_i f$ as before, we have

$$dA = \sqrt{|g|}\, dxdy = \sqrt{1 + f_x^2 + f_y^2}\, dxdy =: \mathcal{L}\, dxdy, \tag{3.16}$$

catenoid

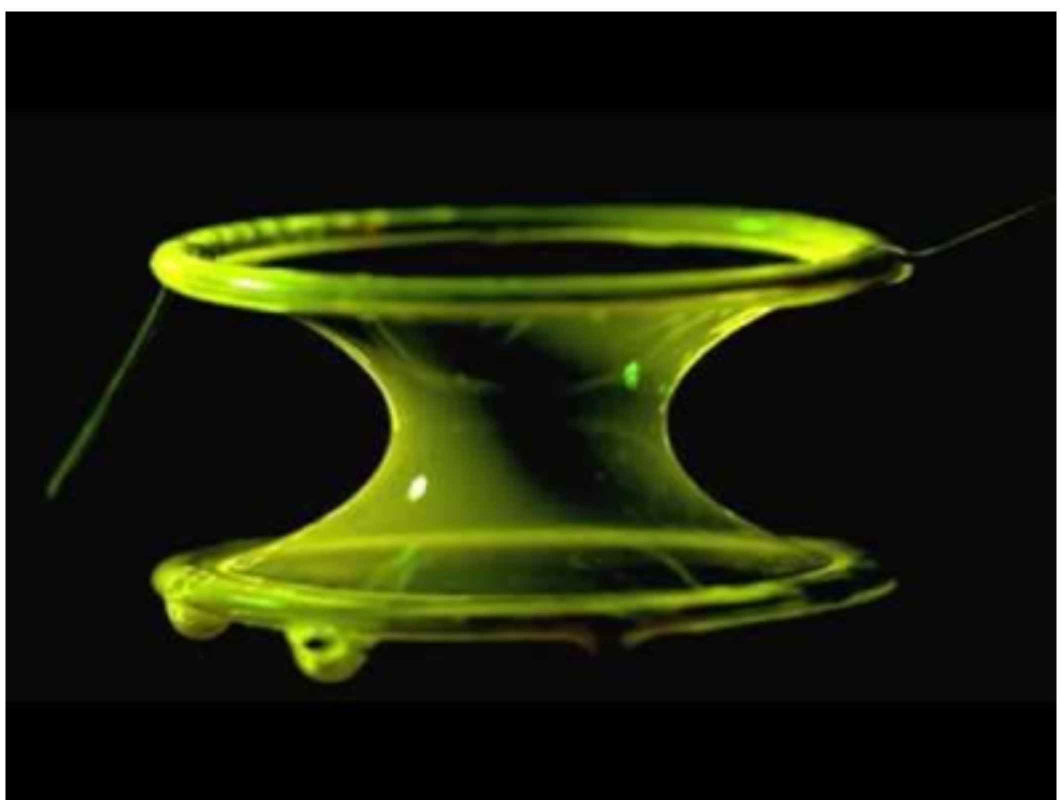

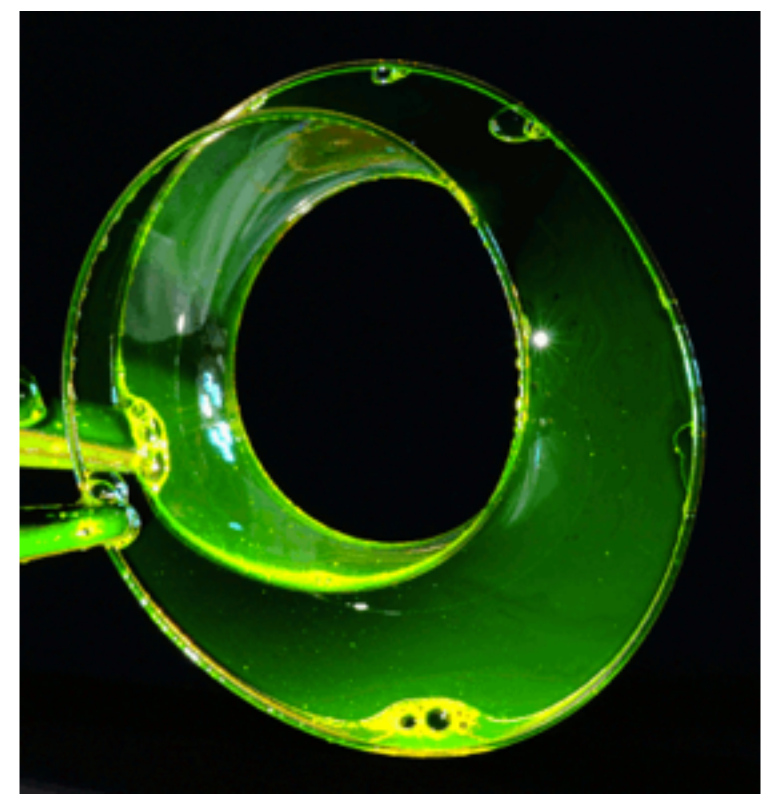

Goldstein lab (Cambridge)

dunkel@math.mit.edu

3.2 Minimal surfaces

Minimal surfaces are surfaces that minimize the area within a given contour ∂M,

$$A(M|\partial M) = \int_M dA = \text{min!} \tag{3.15}$$

Assuming a Cartesian parameterization $z = f(x, y)$ and abbreviating $f_i = \partial_i f$ as before, we have

$$dA = \sqrt{|g|}\, dxdy = \sqrt{1 + f_x^2 + f_y^2}\, dxdy =: \mathcal{L}\, dxdy, \tag{3.16}$$

and the minimum condition (3.15) can be expressed in terms of the Euler-Lagrange equations

$$0 = \frac{\delta A}{\delta f} = -\partial_i \frac{\partial \mathcal{L}}{\partial f_i}. \tag{3.17}$$

Inserting the Lagrangian $\mathcal{L} = \sqrt{|g|}$, one finds

$$0 = -\left[\partial_x \left(\frac{f_x}{\sqrt{1 + f_x^2 + f_y^2}}\right) + \partial_y \left(\frac{f_y}{\sqrt{1 + f_x^2 + f_y^2}}\right)\right] \tag{3.18}$$

which may be recast in the form

$$0 = \frac{(1 + f_y^2) f_{xx} - 2 f_x f_y f_{xy} + (1 + f_x^2) f_{yy}}{(1 + f_x^2 + f_y^2)^{3/2}} = -2H. \tag{3.19}$$

3.2 Minimal surfaces

Minimal surfaces are surfaces that minimize the area within a given contour ∂M,

$$A(M|\partial M) = \int_M dA = \min! \tag{3.15}$$

Assuming a Cartesian parameterization $z = f(x, y)$ and abbreviating $f_i = \partial_i f$ as before, we have

$$dA = \sqrt{|g|}\, dxdy = \sqrt{1 + f_x^2 + f_y^2}\, dxdy =: \mathcal{L}\, dxdy, \tag{3.16}$$

and the minimum condition (3.15) can be expressed in terms of the Euler-Lagrange equations

$$0 = \frac{\delta A}{\delta f} = -\partial_i \frac{\partial \mathcal{L}}{\partial f_i}. \tag{3.17}$$

Thus, minimal surfaces satisfy

$$H = 0 \qquad \Leftrightarrow \qquad \kappa_1 = -\kappa_2, \tag{3.20}$$

implying that each point of a minimal surface is a saddle point.

dunkel@math.mit.edu

3.3 Thermal excitations of almost flat membranes

Assuming that a quasi-infinite membrane prefers a flat configuration, we postulate the energy functional

$$E = \int dA\, f_c\,, \qquad f_c = \frac{k_c}{2}(2H)^2. \tag{3.21a}$$

$$H = \frac{1}{2}\left(\kappa_1 + \kappa_2\right) = \frac{(1+f_y^2)f_{xx} - 2f_x f_y f_{xy} + (1+f_x^2)f_{yy}}{2(1+f_x^2+f_y^2)^{3/2}}$$

The constant k_c is the bending rigidity and carries dimensions of energy. For an almost planar membrane with $|f_x|, |f_y| \ll 1$, we may approximate

$$2H \simeq f_{xx} + f_{yy}, \tag{3.22}$$

which gives to leading order for the energy

$$E \simeq \frac{k_c}{2} \int dxdy\, (f_{xx} + f_{yy})^2. \tag{3.23}$$

dunkel@math.mit.edu

3.3 Thermal excitations of almost flat membranes

$$E \simeq \frac{k_c}{2} \int dxdy\ (f_{xx} + f_{yy})^2. \tag{3.23}$$

Similar to our earlier discussion of polymers, we would like to express the energy in terms of contributions from elementary excitations. To this end, we abbreviate $\boldsymbol{x} = (x, y)$ and consider the Fourier ansatz

$$f(\boldsymbol{x}) = \int \frac{d^2q}{(2\pi)^2}\ \hat{f}_{\boldsymbol{q}}\ \exp(i\boldsymbol{q}\cdot\boldsymbol{x}), \tag{3.24}$$

demanding $\hat{f}_{-\boldsymbol{q}} = \hat{f}^*_{\boldsymbol{q}}$ to ensure real-valued solutions. Inserting the Fourier expansion into (3.23) gives

$$\begin{aligned} E &\simeq \frac{k_c}{2} \int \frac{d^2q}{(2\pi)^2} \int \frac{d^2q'}{(2\pi)^2} \int dxdy\ (i\boldsymbol{q})^2(i\boldsymbol{q}')^2 \hat{f}_{\boldsymbol{q}}\hat{f}_{\boldsymbol{q}'}\ \exp[i(\boldsymbol{q}+\boldsymbol{q}')\cdot\boldsymbol{x}] \\ &= \frac{k_c}{2} \int \frac{d^2q}{(2\pi)^2} \int d^2q'(\boldsymbol{q}^2)(\boldsymbol{q}'^2)\hat{f}_{\boldsymbol{q}}\hat{f}_{\boldsymbol{q}'}\ \delta(\boldsymbol{q}+\boldsymbol{q}') \\ &= \frac{k_c}{2} \int \frac{d^2q}{(2\pi)^2} |\boldsymbol{q}|^4 \hat{f}_{\boldsymbol{q}}\hat{f}_{-\boldsymbol{q}} \\ &= \frac{k_c}{2} \int \frac{d^2q}{(2\pi)^2} |\boldsymbol{q}|^4 \hat{f}_{\boldsymbol{q}}\hat{f}^*_{\boldsymbol{q}}. \end{aligned} \tag{3.25}$$

each bending mode contributes an energy $E(\boldsymbol{q}) \propto |\boldsymbol{q}|^4$

dunkel@math.mit.edu

3.3 Thermal excitations of almost flat membranes

$$E \simeq \frac{k_c}{2}\int \frac{d^2q}{(2\pi)^2}|\boldsymbol{q}|^4 \hat{f}_{\boldsymbol{q}}\hat{f}^*_{\boldsymbol{q}}$$

Two-mode correlation function

$$\begin{aligned}
\langle \hat{f}_{\boldsymbol{q}}\hat{f}^*_{\boldsymbol{q}'}\rangle &= \int D\hat{f}\ \hat{f}_{\boldsymbol{q}}\hat{f}^*_{\boldsymbol{q}'}\ \frac{e^{-\beta E}}{Z} \\
&= \frac{1}{Z}\int D\hat{f}\ \hat{f}_{\boldsymbol{q}}\hat{f}^*_{\boldsymbol{q}'}\ e^{-\beta\frac{k_c}{2(2\pi)^2}\int d^2q d^2q'\ \delta(\boldsymbol{q}-\boldsymbol{q}')|\boldsymbol{q}|^4\hat{f}_{\boldsymbol{q}}\hat{f}^*_{\boldsymbol{q}'}} \\
&= \frac{k_BT}{k_c|\boldsymbol{q}|^4}(2\pi)^2\delta(\boldsymbol{q}-\boldsymbol{q}'). \qquad (3.27)
\end{aligned}$$

---

[1]Recall that for a d-dimensional Gaussian integral with positive-definite diagonal matrix $A = \mathrm{diag}(A_{11},\ldots,A_{dd}) = (A_{ii}\delta_{ij})$

$$\int d^dx\ \left(\frac{\det A}{2\pi}\right)^{1/2} e^{-\frac{1}{2}\boldsymbol{x}\cdot A\cdot\boldsymbol{x}} = 1 \qquad (3.26a)$$

$$\int d^dx\ \left(\frac{\det A}{2\pi}\right)^{1/2} e^{-\frac{1}{2}\boldsymbol{x}\cdot A\cdot\boldsymbol{x}}\ x_ix_j = \frac{\delta_{ij}}{A_{ii}}. \qquad (3.26b)$$

Eq. (3.27) is the infinite-dimensional generalization of this relation, obtained by rewriting the complex path integral in terms of real and imaginary part and by noting that $\int dq'\ \delta(q-q')\ \delta(q'-q'') = \delta(q-q'')$, hence $\delta^{-1} = \delta$ in this sense.

3.3 Thermal excitations of almost flat membranes

$$E \simeq \frac{k_c}{2}\int \frac{d^2q}{(2\pi)^2}|\boldsymbol{q}|^4 \hat{f}_{\boldsymbol{q}}\hat{f}^*_{\boldsymbol{q}}$$

Two-mode correlation function

$$\langle \hat{f}_{\boldsymbol{q}}\hat{f}^*_{\boldsymbol{q}'}\rangle = \frac{k_BT}{k_c|\boldsymbol{q}|^4}(2\pi)^2\delta(\boldsymbol{q}-\boldsymbol{q}')$$

This result can be used to calculate the thermal mean squared deviations of the derivatives

$$\begin{aligned}
\langle f_x^2 + f_y^2\rangle &= -\int \frac{d^2q}{(2\pi)^2}\int \frac{d^2q'}{(2\pi)^2}\,(\boldsymbol{q}\cdot\boldsymbol{q}')\langle \hat{f}_{\boldsymbol{q}}\hat{f}^*_{\boldsymbol{q}'}\rangle \\
&= -\int \frac{d^2q}{(2\pi)^2}\int \frac{d^2q'}{(2\pi)^2}\,(\boldsymbol{q}\cdot\boldsymbol{q}')\frac{k_BT}{k_c|\boldsymbol{q}|^4}(2\pi)^2\delta(\boldsymbol{q}-\boldsymbol{q}') \\
&= \int \frac{d^2q}{(2\pi)^2}\frac{k_BT}{k_c|\boldsymbol{q}|^2} \\
&= \int \frac{d|\boldsymbol{q}|}{2\pi}\frac{k_BT}{k_c|\boldsymbol{q}|},
\end{aligned} \tag{3.28}$$

3.3 Thermal excitations of almost flat membranes

$$E \simeq \frac{k_c}{2}\int \frac{d^2q}{(2\pi)^2}|\boldsymbol{q}|^4 \hat{f}_{\boldsymbol{q}}\hat{f}^*_{\boldsymbol{q}}$$

Two-mode correlation function

$$\langle \hat{f}_{\boldsymbol{q}}\hat{f}^*_{\boldsymbol{q}'}\rangle = \frac{k_BT}{k_c|\boldsymbol{q}|^4}(2\pi)^2\delta(\boldsymbol{q}-\boldsymbol{q}')$$

$$\langle f_x^2 + f_y^2\rangle = \int \frac{d|\boldsymbol{q}|}{2\pi}\frac{k_BT}{k_c|\boldsymbol{q}|}$$

Need to introduce cut-offs !

$$\langle f_x^2 + f_y^2\rangle = \frac{k_BT}{2\pi k_c}\int_{(2\pi)/L}^{(2\pi)/a}\frac{d|\boldsymbol{q}|}{|\boldsymbol{q}|} = \frac{k_BT}{2\pi k_c}\ln(L/a). \tag{3.29}$$

Recalling our initial assumption $|f_x|, |f_y| \ll 1$, we see that the notion of planar membrane is only meaningful as long as $\langle f_x^2 + f_y^2\rangle \ll 1$, or equivalently if

$$L \ll L_P = ae^{2\pi k_c/(k_BT)}, \tag{3.30}$$

where L_P is the persistence length, defined by the condition $\langle f_x^2 + f_y^2\rangle = 1$.

dunkel@math.mit.edu

3.4 Helfrich's model

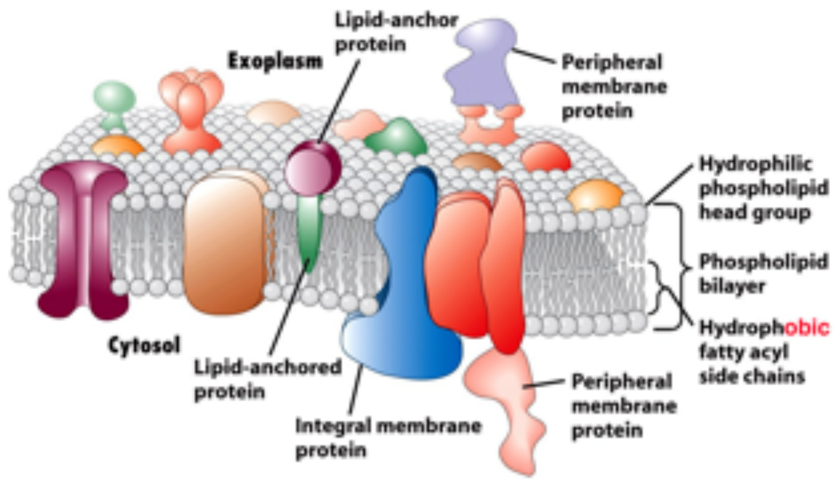

Figure 10-1
Molecular Cell Biology, Sixth Edition
© 2008 W.H. Freeman and Company

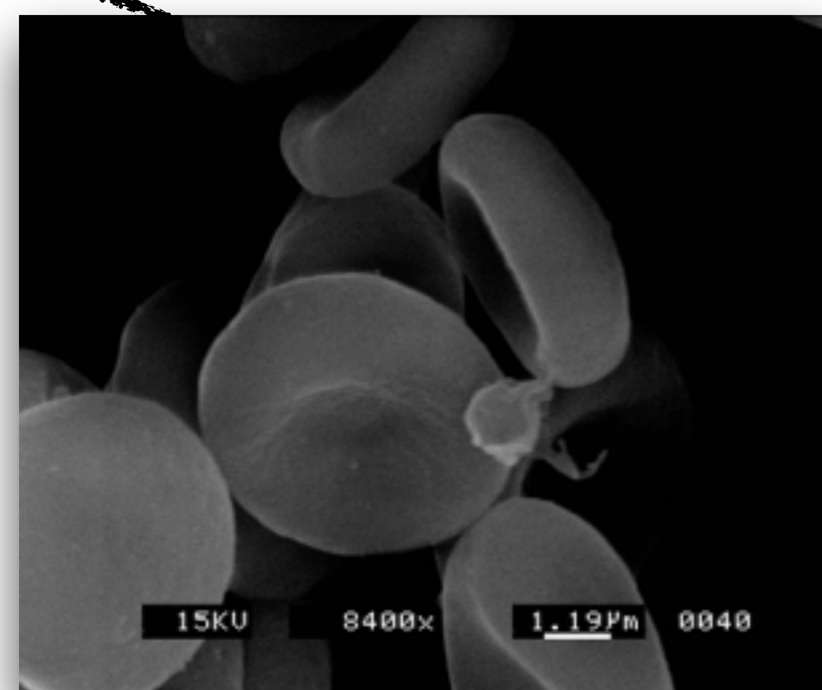

wiki

www.math.tamu.edu/~bonito/

dunkel@math.mit.edu

3.4 Helfrich's model

Assuming that lipid bilayer membranes can be viewed as two-dimensional surfaces, Helfrich [Hel73] proposed in 1973 the following geometric curvature energy per unit area for a closed membrane

$$f_c = \frac{k_c}{2}(2H - c_0)^2 + k_G\, K, \tag{3.31}$$

where constants k_c, k_G are bending rigidities and c_0 is the spontaneous curvature of the membrane. The full free energy for a closed membrane can then be written as

$$F_c = \int dA\, f_c + \sigma \int dA + \Delta p \int dV, \tag{3.32}$$

where σ is the surface tension and Δp the osmotic pressure (outer pressure minus inner pressure). Minimizing F with respect to the surface shape, one finds after some heroic manipulations the shape equation[2]

$$\Delta p - 2\sigma H + k_c(2H - c_0)(2H^2 + c_0 H - 2K) + k_c \nabla^2(2H - c_0) = 0, \tag{3.33}$$

where ∇^2 is the Laplace-Beltrami operator on the surface. The derivation of Eq. (3.33) uses our earlier result

$$\frac{\delta A}{\delta f} = -2H, \tag{3.34}$$

and the fact that the volume integral may be rewritten as[3]

$$V = \int dV = \int dA\, \frac{1}{3} \boldsymbol{F} \cdot \boldsymbol{N}\ , \tag{3.35}$$

$dV = \frac{1}{3} h\, dA$ for a cone or pyramid of height $h = \boldsymbol{F} \cdot \boldsymbol{N}$

3.4 Helfrich's model

Assuming that lipid bilayer membranes can be viewed as two-dimensional surfaces, Helfrich [Hel73] proposed in 1973 the following geometric curvature energy per unit area for a closed membrane

$$f_c = \frac{k_c}{2}(2H - c_0)^2 + k_G\, K, \tag{3.31}$$

where constants k_c, k_G are bending rigidities and c_0 is the spontaneous curvature of the membrane. The full free energy for a closed membrane can then be written as

$$F_c = \int dA\, f_c + \sigma \int dA + \Delta p \int dV, \tag{3.32}$$

where σ is the surface tension and Δp the osmotic pressure (outer pressure minus inner pressure). Minimizing F with respect to the surface shape, one finds after some heroic manipulations the shape equation[2]

$$\Delta p - 2\sigma H + k_c(2H - c_0)(2H^2 + c_0 H - 2K) + k_c \nabla^2 (2H - c_0) = 0, \tag{3.33}$$

where ∇^2 is the Laplace-Beltrami operator on the surface. The derivation of Eq. (3.33) uses our earlier result

$$\frac{\delta A}{\delta f} = -2H, \tag{3.34}$$

and the fact that the volume integral may be rewritten as[3]

$$V = \int dV = \int dA\, \frac{1}{3}\boldsymbol{F} \cdot \boldsymbol{N}\ , \tag{3.35}$$

$$\Rightarrow \quad \frac{\delta V}{\delta f} = 1.$$

3.4 Helfrich's model

Assuming that lipid bilayer membranes can be viewed as two-dimensional surfaces, Helfrich [Hel73] proposed in 1973 the following geometric curvature energy per unit area for a closed membrane

$$f_c = \frac{k_c}{2}(2H - c_0)^2 + k_G\, K, \tag{3.31}$$

where constants k_c, k_G are bending rigidities and c_0 is the spontaneous curvature of the membrane. The full free energy for a closed membrane can then be written as

$$F_c = \int dA\, f_c + \sigma \int dA + \Delta p \int dV, \tag{3.32}$$

where σ is the surface tension and Δp the osmotic pressure (outer pressure minus inner pressure). Minimizing F with respect to the surface shape, one finds after some heroic manipulations the shape equation[2]

$$\Delta p - 2\sigma H + k_c(2H - c_0)(2H^2 + c_0 H - 2K) + k_c \nabla^2 (2H - c_0) = 0, \tag{3.33}$$

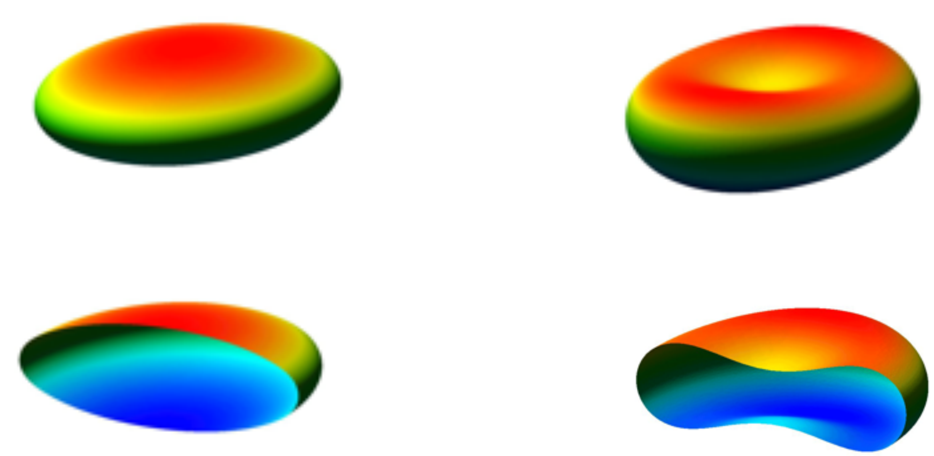

www.math.tamu.edu/~bonito/

dunkel@math.mit.edu

3.4 Helfrich's model

Assuming that lipid bilayer membranes can be viewed as two-dimensional surfaces, Helfrich [Hel73] proposed in 1973 the following geometric curvature energy per unit area for a closed membrane

$$f_c = \frac{k_c}{2}(2H - c_0)^2 + k_G\, K, \tag{3.31}$$

where constants k_c, k_G are bending rigidities and c_0 is the spontaneous curvature of the membrane. The full free energy for a closed membrane can then be written as

$$F_c = \int dA\, f_c + \sigma \int dA + \Delta p \int dV, \tag{3.32}$$

For open membranes with boundary ∂M, a plausible energy functional is given by

$$F_o = \int dA\, f_c + \sigma \int dA + \gamma \oint_{\partial M} ds, \tag{3.37}$$

where γ is the line tension of the boundary. In this case, variation yields not only the corresponding shape equation but also a non-trivial set of boundary conditions.

dunkel@math.mit.edu